2012-06-06

Structural Properties of ICLT Wall Panels Composed of Beetle Killed Wood

David Edward Wilson
Brigham Young University - Provo

Structural Properties of ICLT Wall Panels

Composed of Beetle Killed Wood

David Edward Wilson II

A thesis submitted to the faculty of
Brigham Young University
in partial fulfillment of the requirements for the degree of

Master of Science

Fernando S. Fonseca, Chair
Richard J. Balling
Paul W. Richards

Department of Civil & Environmental Engineering

Brigham Young University

June 2012

ABSTRACT

Structural Properties of ICLT Wall Panels
Composed of Beetle Killed Wood

David Edward Wilson II
Department of Civil & Environmental Engineering, BYU
Master of Science

Interlocking Cross Laminated Timber (ICLT) wall panels are a new wood construction product similar to Cross Laminated Timber panels. Besides being an innovative structural system, they also utilize beetle killed timber from many of the forests that have been devastated by the Mountain Pine Beetle.

Three tests were performed on three ply ICLT panels measuring 8 feet (2.44m) wide, 8 feet (2.44m) tall and 8.5 inches (21.6cm) thick to determine the racking, flexural and axial strengths of the wall panels. After each test was performed the walls were disassembled and investigated for cause of failure. Using the data from the tests as a benchmark, simple analytical models to predict the design capacities of the walls for racking, flexural, and axial strengths were established. The analytical models for racking strength, flexural strength and axial strength predicted reasonably well the measured strength values. Additional testing is necessary to increase the available database, further validate the analytical models developed, better understand the structural performance of ICLT panels, and establish acceptable design methodology for ICLT wall panels.

Keywords: ICLT, beetle killed, blue stain, mechanical properties, analytical model, racking strength, flexural strength compressive strength

ACKNOWLEDGMENTS

I would like to take this opportunity to thank my adviser Fernando S. Fonseca for his continual guidance during my master's program. I would like to thank Euclid Timber Frames for coming up with the ICLT design and providing the walls. I would also like to express my appreciation to Dave Anderson, Rodney Mayo and their lab technicians that helped to build the testing frames and run the tests. Lastly I would like to thank my wife and my family for always supporting me and giving me an ear to talk through my research with.

TABLE OF CONTENTS

LIST OF TABLES

LIST OF FIGURES

1 INTRODUCTION

As the world has been moving toward a more sustainable model for structural design there have been many innovations to materials and designs. One of these innovations was the development of Interlocking Cross Laminated Timber (ICLT) panels. These multi-layer wooden panels utilize beetle killed waste wood and use dovetail and tongue and grove connections to keep the wall together.

The ICLT panel is a new product and is still in the beginning stages of development. A proof of concept study performed by Steven Sanders (Sanders 2011) is the only other structural testing performed on ICLT panels to date. Sanders proof of concept study tested a five ply ICLT panel in an in-plane lateral load test and compared its racking strength to those of traditional wooden stick frame construction, and Cross Laminated Timber (CLT) panels. He found that the racking strength of ICLT panels is twice as strong as CLT panels in the elastic range and an order of magnitude stronger than stick framing (Sanders 2011). Sanders proof of concept research clearly showed the racking strength and potential of ICLT panels as a building material.

This thesis is a pilot program to develop simplified analytical models for racking strength, flexural strength and axial strength of ICLT panels. The research will be performed in two steps. The first of these steps will be to conduct additional structural tests on three-ply ICLT wall panels to increase the database. These tests will include an in-plane lateral load test, an out-

of-plane load test and an in-plane vertical load test. The second step will be to use the results from these tests to develop simple analytical models for racking, flexural and axial compressive strengths of ICLT panels, respectively. Ideally these analytical models will be further validated and then used for design purposes.

Testing the wall panels in three different ways will serve as a stepping stone for further and more refined research in ICLT design. The thesis will address the above mentioned steps in the following manner:

- A brief history of the Cross Laminated Timber (CLT) and ICLT innovations and the use of beetle killed wood in making these wood panels is given in Chapter 2.
- A description of the set up and testing procedure of the three tests performed on the three-ply ICLT wall panels is provided in Chapter 3.
- A presentation of the results from the three-ply ICLT wall panel tests is given in Chapter 4.
- A discussion on the results of the research done by Uyema (Uyema 2012) on the material properties of the beetle killed wood and the relevance of those results to the current research are presented in Chapter 5.
- A presentation on the use of beetle killed material properties in calculating overall wood panel strengths is developed in Chapter 6.
- The conclusions from this research are provided in Chapter 7.

2 BRIEF HISTORY OF CLT AND ICLT PANELS AND MOUNTAIN PINE BEETLE

Cross laminated timber (CLT) panels are a relatively new form of construction in the United States with many different building codes still adding provisions for CLT design. ICLT panels are an even newer product that is just starting to be used as a construction system. Tests are still being performed on ICLT panels. A brief introduction to CLT and ICLT panels is given below. A short description of the process and effects of a Mountain Pine Beetle attack is also included.

2.1 CLT and ICLT Panels

As the demand for sustainable structures has increased around the world many new and innovative products and designs have been created. The ICLT wall panels are a new sustainable design that utilizes beetle killed timber harvested from the United States and Canada. This design was inspired by the CLT design. Cross laminated timber panels originated in Austria as a way to utilize the scrap wood produced from milling conventional lumber (Sanders 2011). The panels are configured like giant pieces of ply wood where parallel boards are glued side by side in a single layer and then glued to another layer of boards placed orthogonal to the initial layer as shown in Figure 2-1. The panels commonly range from three to nine layers, creating a panel ranging from 3.9 inches (9.9cm) to 12.2 inches (31cm) thick (Structurlam 2010).

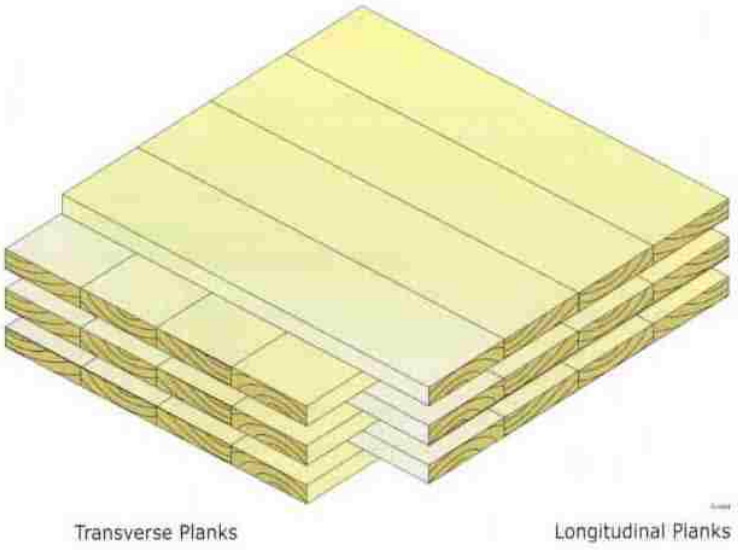

Figure 2-1: Layout of Individual Boards to Form CLT Panels, (FPInnovations 2011)

The use of CLT panels has become a popular method of construction for all kinds of structures ranging from churches and barns to low rise apartment and office buildings. Perhaps the most notable of these structures is the Stadthaus building in the United Kingdom. The Stadthaus building is the world's tallest mixed-use wood structure with eight floors of CLT construction sitting on one floor of cast concrete (Ward 2009).

There are many advantages to using CLT panels for construction. Cross laminate timber panels have much greater strength than conventional stick framing, are much lighter than steel or concrete construction, and are made traditionally from an underutilized resource. The speed of construction with CLT panels is fast due to the fact the panels themselves are prefabricated to include door and window frames and can even include electrical conduits (Smith 2011). However there are two notable disadvantages: (1) the adhesive used for CLT panels is often toxic or if adhesives are not used many mechanical fasteners are required to hold the layers

together and (2) once a panel is assembled with adhesive it cannot be disassembled to be reused (Smith 2011). The ICLT panels have all the advantages of the CLT panels without the disadvantages. What makes an ICLT panel unique are the interlocking dovetail pieces. These dovetail boards interlock with the adjacent layers much like the pieces of a puzzle. The interlocking process removes the need for mechanical fasteners or toxic adhesives to hold the panels together. The layout of an ICLT panel including dovetail boards (blue boards) can be seen in Figure 2-2. For a more detailed description of the ICLT panel layout and construction methods, see Sanders (Sanders 2011). The other advantage of the ICLT system is that an ICLT panel can be disassembled after its useful life and the individual wood pieces are once again a reusable resource (Smith 2011).

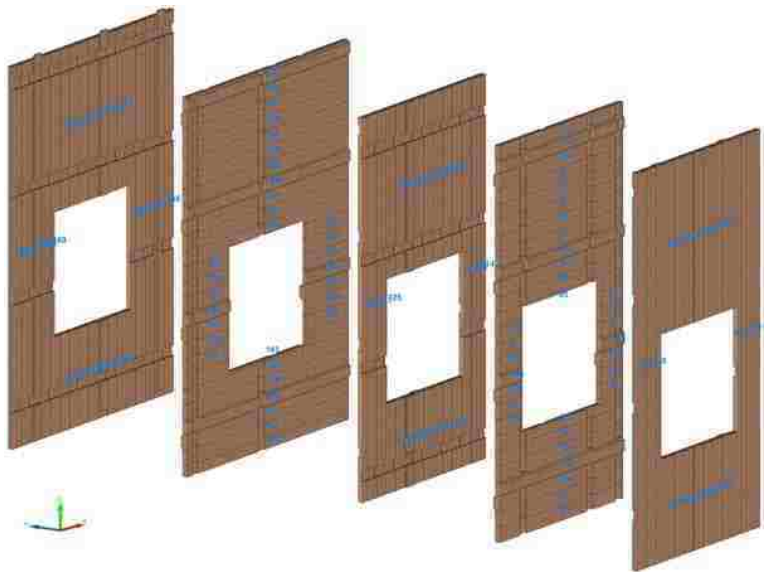

Figure 2-2: Layout of ICLT Panel with Window Cutout (Apostol 2011)

2.2 **Mountain Pine Beetle**

One of many reasons why much of the United States forests are not as healthy as they used to be is from Mountain Pine Beetle (MPB) attacks. In 2010 over 9.4 million acres ($3.8x10^{10}$ m^2) of United State forest land was killed by beetles and disease, 74% of that was killed by the MPB, *Dendroctonus ponderosae* (USDA 2011). During a normal outbreak the MPB will attack stressed or unhealthy large diameter pine trees, but during larger outbreaks MPB will often attack trees regardless of the tree diameter. The MPB attacks by boring into the tree truck just below the bark in the mid to late summer and lay a nest of eggs in a long vertical tube. The eggs hatch before winter and larva live out that winter in the tree before emerging as beetles in the mid to late summer and starting the entire process over again (Leatherman et al. 2007). Many beetles may attack the same tree increasing the probability of killing the tree. The beetle tunnels can cut off nutrient transfer in the sapwood of the tree, and in addition, the MPB carries a fungus. This fungus feeds on the sugars and carbohydrates found in the trees sap wood. It is evident the fungus is present in the tree by the bluish or grayish discoloration of the trees' sapwood. Once the tree is robbed of its nutrients it begins to die (Knaebe 2002). Although not a requirement of necessity, ICLT panels are currently being constructed from this underutilized waste wood.

3 ICLT WALL TEST SETUP AND PROCEDURE

In order to gain a better understanding of the performance of the ICLT walls, three tests were performed. The first test was an in-plane lateral load to determine the racking strength of the wall. The second test was an out-of-plane loading test to determine the flexural strength of the wall. The third test was an in-plane vertical load to determine the axial strength of the wall. Detailed descriptions of these three tests follow below.

3.1 In-Plane Lateral Load Test

The in-plane lateral load test was performed to gather information on the racking strength of the wall. This was done by attaching the bottom edge of the wall to a frame while the top edge was allowed to move parallel with the length of the wall.

3.1.1 Testing Frame

The reaction frame was composed of a vertical W12x72 column with two W8x31 braces. The frame was anchored to the ground using three, 2.0 inch (5.08cm) DYWIDAG bars post-tensioned to the floor, one bar in each steel brace member.

A loading frame was constructed from two sidesway frames composed of two W8x31 columns connected near the top with a specialty built H-frame composed of two HSS6x3x3/8 tubes with two smaller sections of the same tubing welded to them forming a small square at the

middle of the H-frame. This allowed for a sliding arm composed of two parallel HSS4x2x3/8 held 1.625 inches (4.13cm) apart by welded steel plates on the ends. The sliding arm slides freely through openings of the H-frames. A specialty built cap composed of a ST9x27.35 welded to the back web face of a C15x33.9 structural channel was designed to be able to move freely in the 1.625 inch (4.13cm) gap of the sliding arm. The cap had a reinforced vertical grove in the arm of the ST9x27.35 section that allows in-plane rotation of the wall during testing. This sliding arm attached to the cap using a centralized pin placed through the sliding arm and grove in the cap. The testing frame and set-up is shown in Figure 3-1.

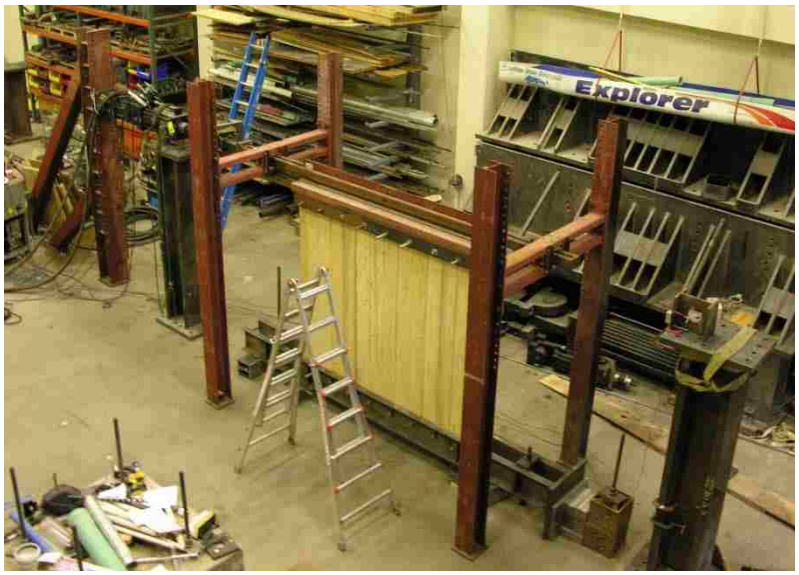

Figure 3-1: In-Plane Lateral Load Test Frame and Setup with an ICLT Wall in Place

The bottom of the wall was held by sandwiching the base of the wall with two C12x25 channels. The wall was attached to the channels with eight, 1.0 inch (2.54cm) diameter all-thread bolts at 12 inches (30.48cm) on center going through the entire thickness of the wall and channel sandwich. The channels and wall system was held off the floor by two reinforced

W8x67 I-beam spacers. The top of the wall was attached to the cap with a similar configuration as that of the bottom with eight 1.0 inch (2.54cm) diameter all-thread bolts going through the wall. Rather than channels, two 0.375 inch (9.5mm) steel plates were welded to the flange portions of the cap. Due to the width of the top connecting system, 4x4 wood spacers were needed on both sides of the wall for a tight connection. The entire test frame and setup with an ICLT wall in place is shown in Figure 3-1.

3.1.2 Test Procedure

The loading for the test was applied using an MTS 100 kip, 20 inch (444.8kN, 50.8cm) hydraulic actuator. The actuator was connected to both the sliding arm and vertical portion of the reaction frame. The test was performed at a loading rate 0.2 in/min (5mm/min) and a scanning speed of 1 scan/sec. To gather wall deflection information for the test, five string potentiometers (string pots) were used. The wall was set up in a west to east direction with the actuator on the west side of the wall. String pots 1 and 2 were placed on the bottom of the wall in both the west and east corners to measure any possible vertical movement of the wall. String pots 3 and 4 were placed on the top and bottom of the east edge of the wall in order to measure the lateral movement or drift of the wall. String pot 5 was attached to the plate welded between the double channels on the bottom of the wall to measure any possible horizontal sliding movement of the bottom frame. A drawing of the placement of string pots with respect to the wall is shown in Figure 3-2.

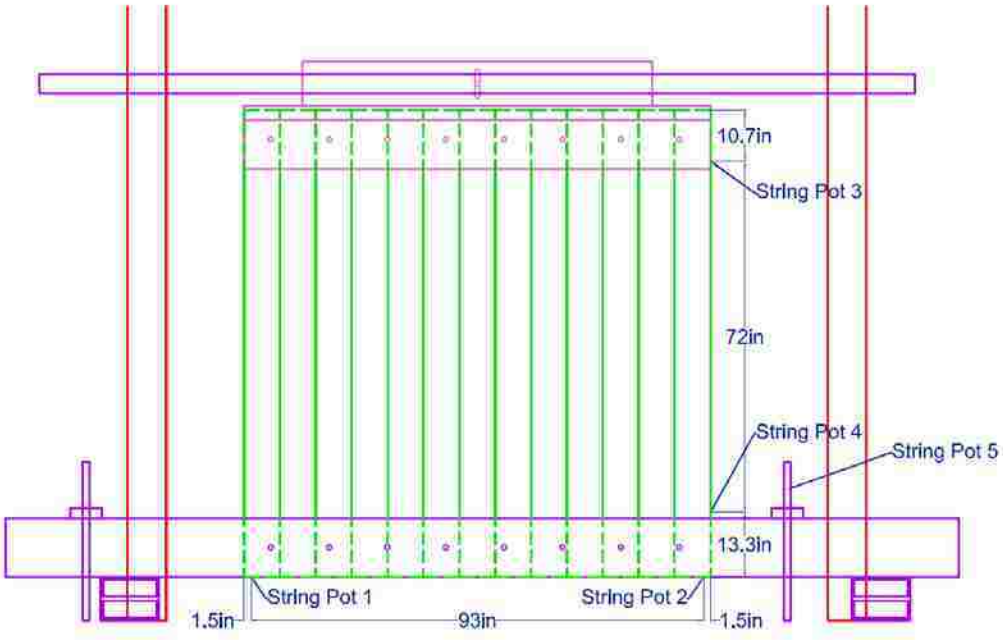

Figure 3-2: String Pot Locations for In-Plane Lateral Load Test

3.2 Out-of-Plane Loading Test

The out-of-plane loading or flexural test was performed on one of the walls orientated such that the outer layers of the three ply system resisted the load: one in compression (the top layer) and one in tension (the bottom layer). The wall was laid horizontally in a four point layout with two line loads along the width of the wall at the third points and two supports 3.0 inches from the edge of the bottom layer of the wall.

3.2.1 Testing Frame

The flexure test reaction frame was constructed using a simple beam and column design with a 2000 kip (8.89MN) capacity. The columns consisted of two sections of W14x398 steel

shapes spliced together using 13, 1.5 inch (3.81cm) diameter A490 bolts. Each bottom column section was anchored to the structural floor by post-tensioning four, 2.0 inch (5.08cm) DYWIDAGs. The base of the column was capped with a frame made of HSS10x10x5/8 tubing to act as a “giant” washer for the four DYWIDAG bars and to match the hole pattern in the structural floor. The top section of the column has been permanently welded to the top beam. The top beam was constructed in a reinforced L-shape, from 2.25 inch (5.7cm) steel plate. The loading frame was built from an HSS10x10x5/8 tube welded to the flange portion of two C10x30 steel channels forming an H-shape. The channels were spaced 29.75 inches (75.6cm) on center. The bottom flange had a 1.25 inch (3.18cm) standard pipe welded to it to apply the distributed load along the 8.0 foot (2.44m) length of the wall. The two channels were braced using steel angles intermittently welded to the channels webs along the length of the H-frame. A support frame was constructed from two W12x40 beams spaced 89 inches (2.26m) on center. A 1.25 inch (3.18cm) standard pipe was also welded to the top of each W12x40 beam to act as support. In order to have the necessary pushing distance for the actuator, the beams were elevated off the ground by reinforced steel spacers made from 1.0 foot (30.5cm) sections of W12x40 steel beams. The entire supporting frame was anchored to the floor using 1.25 inch (3.18cm) DYWIDAGs as well as welding it to the reaction frame where possible. The entire test setup with an ICLT wall in place is shown in Figure 3-3.

3.2.2 Test Procedure

The same MTS 100 kip, 20 inch (444.8kN, 50.8cm) hydraulic actuator from the in-plane lateral load test was used on this test. The actuator was attached to the top beam of the reaction frame and to the HSS10x10x5/8 steel tubing of the loading frame. The test was performed at 0.2

in/min (5mm/min) and a sampling rate of one sample/sec. The loading H-frame was built to apply two line loads at third points along the top face of the wall. The outer layers of the wall were orientated perpendicular to the line loads. The wall was placed horizontally on top of the supporting frame such that the outer boards of the ICLT wall were arranged perpendicular to the supporting beams. Seven string pots and two linear variable differential transformers (LVDTs) were used to determine deflections of the wall. String pots numbers 1 through 4 were placed on each end of the two pipes used to apply the line loads to the wall. These string pots were used to measure any differential deflection of the loading apparatus. String pots 5 through 7 were placed equidistantly in the middle of the underside of the wall running parallel to the line loads. These were used to measure the midspan deflection of the wall. The LVDTs number 1 and 2 were used to measure any lateral deflection of the support frame. A drawing of the string pot locations is shown in Figure 3-4.

Figure 3-3: Out-of-Plane Load Test Setup with an ICLT Wall in Place

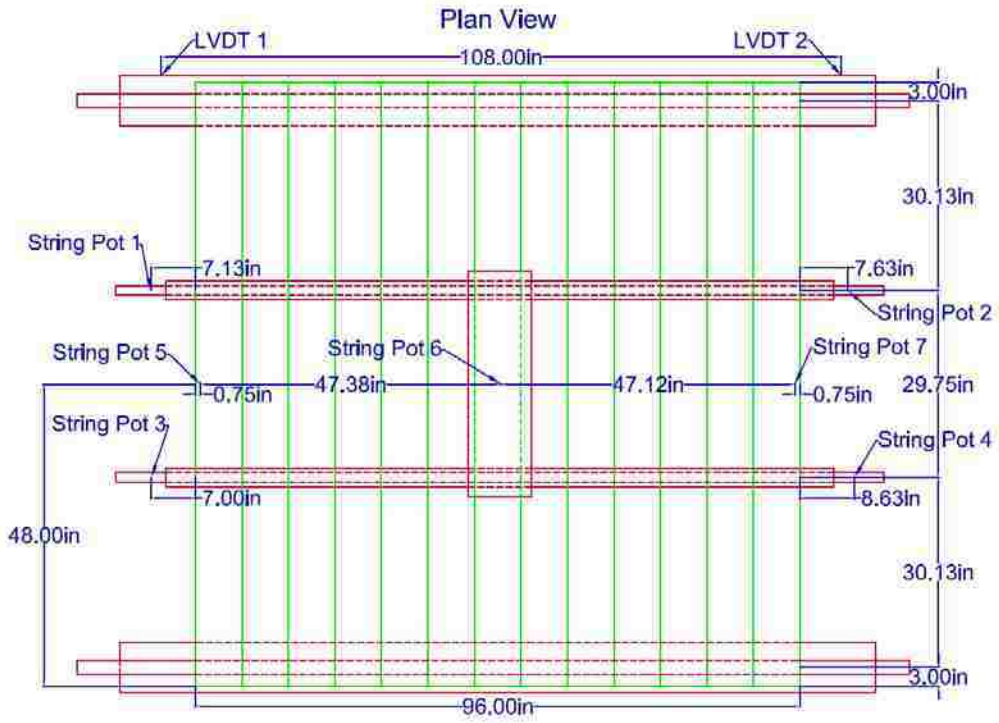

Figure 3-4: String Pot Locations for Out-of-Plane Loading Test, Looking Down

3.3 In-Plane Vertical Load Test

The axial loading test was performed in order to obtain the vertical compressive strength of the walls. Due to the configuration of the wall, the two outer layers were arranged vertically and most likely resisted the vast majority if not all the load. Precautions were taken to remove or minimize any eccentricity from the loading system and to apply a uniform distributed load to the wall.

3.3.1 Testing Frame

The reaction frame for the axial compression test was the same frame used in the out-of-plane loading test with two minor differences. The entire frame was lifted on top of two 18 inch (45.7cm) steel stub columns, one under each column. The reaction frame also had two stiffened

C12x25 steel channels welded to either side of the columns approximately 102 inches (2.6m) off the ground. These channels were attached to keep the loading frame from moving laterally out-of-plane and eliminate or minimize the eccentricity, if any, of the load.

The loading frame for this test was comprised of a W12x87 steel beam with web stiffeners made from 0.375 inch (9.5mm) steel plate 8.0 inches (20.3cm) on center along the length of the beam on both sides. The beam was also capped with a 5.0 inch (12.7cm) solid steel spacer in the middle of the beam where the swivel head for the test was attached. The wall was seated vertically in a C10x30 steel channel, which was held in place from lateral movement by four steel box spacers anchored to the structural floor with 1.5 inch (3.81cm) DYWIDAG bars and 1.0 inch (2.54cm) plywood spacers running along the entire length of the channel. The entire test setup with ICLT wall in place is shown in Figure 3-5.

Figure 3-5: In-Plane Vertical Load Test Setup with an ICLT Wall in Place

3.3.2 Test Procedure

Due to the expected compressive strength of the wall, the load was applied by a Power Team 500 ton, 13 inch (4.45MN, 33cm) hydraulic jack. A Geokon 3000 load cell was placed in line with the jack for this test. Load and deflection readings were taken at two samples per second. To help assure a uniform distributed applied load on the wall, a neoprene layer was placed between the top of the wall and the W12x87 steel beam of the loading frame. A total of twelve string pots and two LVDTs were used to measure deflections for this test. Four of the string pots, numbers 1 and 2 on the north face and numbers 5 and 6 on the south face were used at the top of the wall to measure the vertical deflection as the wall was seated. String pots number 9 and 10 and LVTDs number 1 and 2 were placed in the same orientation but at the bottom of the wall to measure the seating deflection at the bottom of the wall. String pots number 3 and 4 on the north face and numbers 7 and 8 on the south face were attached half way up the face of the wall to measure out-of-plane deflection. These last four sting pots were placed half way up the wall in the center of the outer layer dovetail boards. This was done due to the overall importance of these boards to the structural integrity of the ICLT wall. String pots number 11 and 12 were attached to each of the loading frame beam's overhanging edges to measure the overall vertical deflection of the wall. Drawings of the locations of the string pots and LVDTs for the north and south faces of the wall is shown in Figure 3-6 and Figure 3-7, respectively.

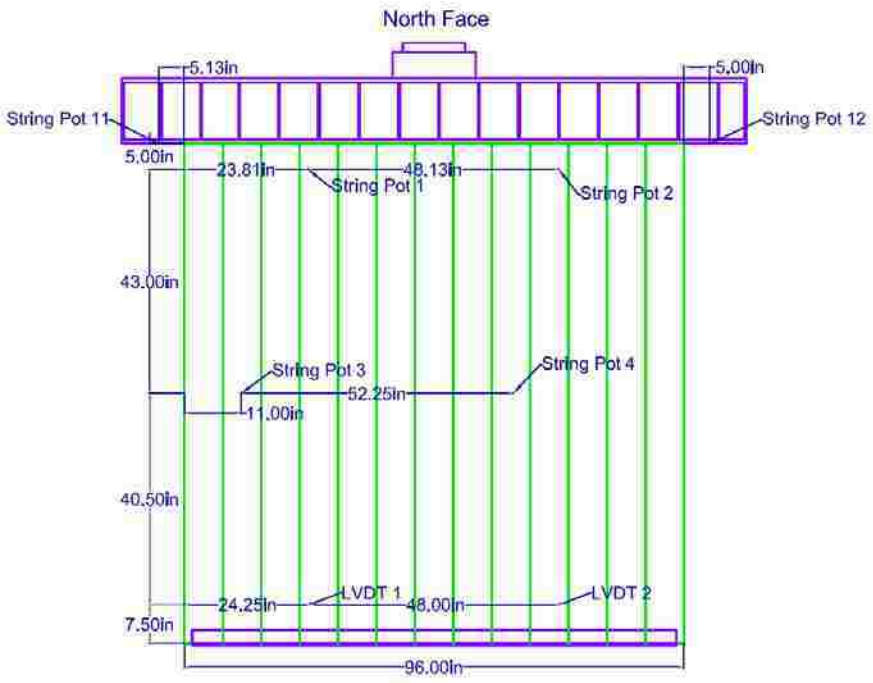

Figure 3-6: String Pot Locations for the In-Plane Vertical Load Test, North Face

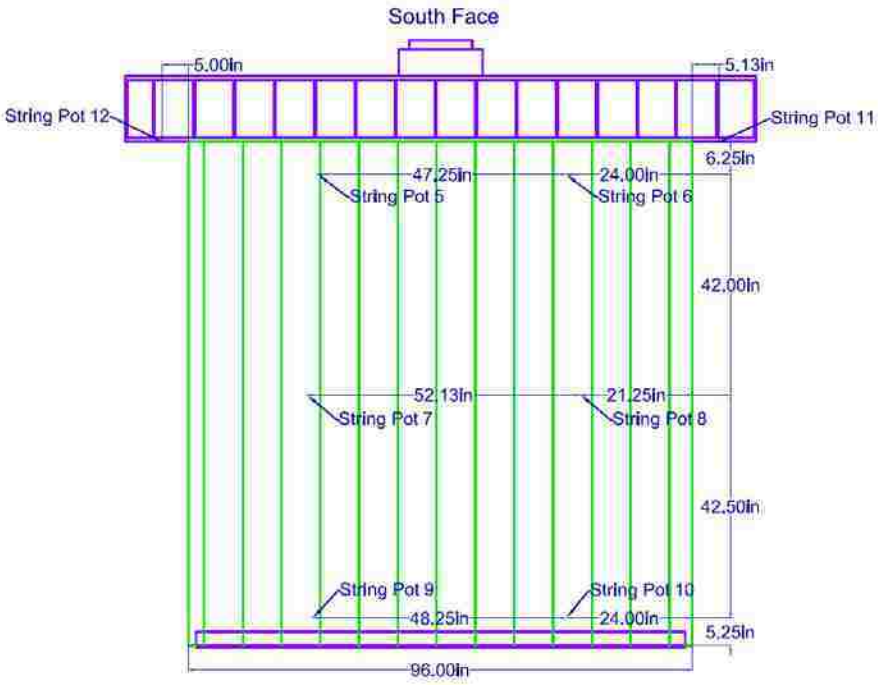

Figure 3-7: String Pot Locations for the In-Plane Vertical Load Test, South Face

4 RESULTS OF ICLT WALL TESTS

After the tests were completed the data was analyzed and the walls dismantled to inspect how the walls moved during the tests, and what type of failures occurred within the wall. These observations and the results of the tests are recorded below.

4.1 In-Plane Lateral Load Test Results

The in-plane measured response of the walls drift is shown in Figure 4-1. The deflection measurements used in Figure 4-1 is from the difference of string pots number 3 and 4. In the in-plane lateral loading configuration the ICLT wall showed a lot of flexibility as well as sustained strength. The wall was tested to a maximum load of 33.3 kips (148.1kN) and the overall deflection at the top of the wall was 11 inches (27.9cm). The maximum story drift was 8.45 inches (21.7cm). The test was stopped due to the reaching of the displacement limits on the hydraulic actuator. The wall sustained a 13 kip (57.8kN) load when meeting the code drift limit of 0.025h (Engineers 2010). That equates to 1.8 inches (4.6cm) of drift for the 72 inch (1.83m) span between string pots number 3 and 4 measuring the horizontal deflection of the wall. The load would equate to a static lateral load of 1.625 kips/ft (23.7kN/m) over the eight foot (2.44m) length of the wall. Calculations are provided in Appendix D. At this load, as shown in Figure 4-1, the wall would have already sustained permanent lateral deflections.

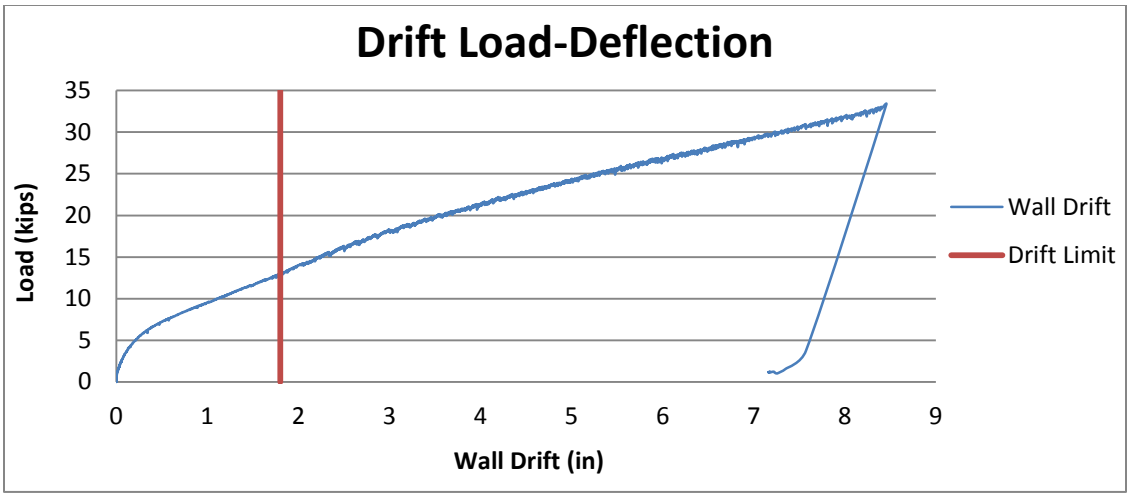

Figure 4-1: Load-Deflection Curve of Wall Drift for In-Plane Lateral Load Test

During the test the wall gained strength (with increased displacement) from the interlocking boards binding with each other. Upon dismantling the wall it became apparent that the wall experienced from crushing at the male-female connection of the dovetail boards. As shown in Figure 4-2, the dovetail board has a kind of zipper pattern along each edge. The pattern is a result of one of the edges of a vertical interlocking board crushing into the dovetail section of a horizontal member while the opposite edge opened. Each one of these crushing marks was 0.1875 to 0.25 inches (4.7mm-6.4mm) deep. Collectively the wall had 196 of these crushing marks distributed between eight dovetail members. Other forms of damage experienced by the wall were at the wall-to-frame connections. At each of the eight, 1.0 inch (2.54cm) diameter all-thread bolts used to attach the bottom of the wall, severe elongation of the holes were observed. The "stretching" of the holes and 0.5 inches (1.27cm) of deflection of the bottom frame translated into 2.0 inches (5.08cm) of total lateral movement at the base of the wall. Figure 4-3 shows the elongation of one of the holes through the bottom of the wall. The large measured wall displacements are most likely due to the amount of connections in the wall and the movement

experienced by each of those connections. Additional tables, figures and load-deflection curves corresponding to the in-plane lateral load test are found in Appendix A.

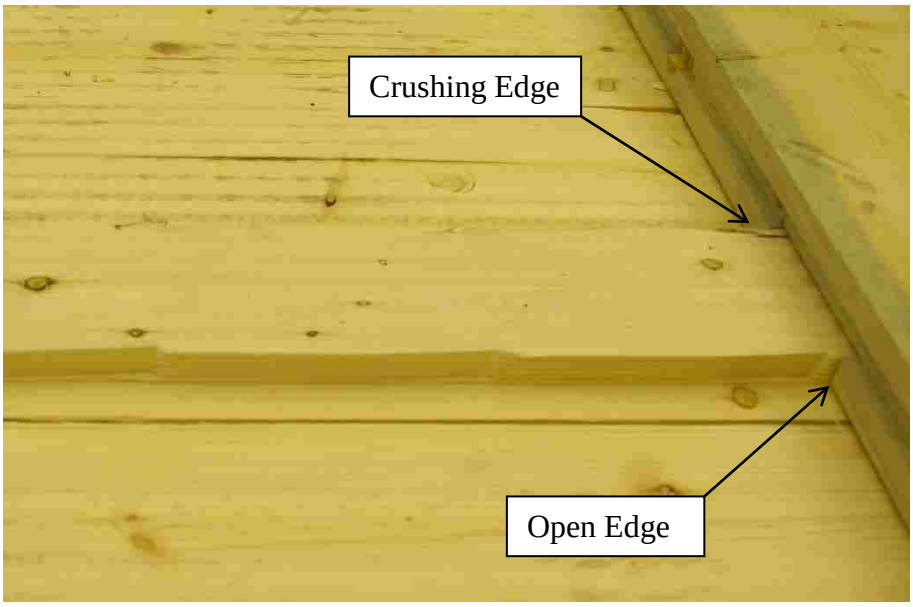

Figure 4-2: Crushing Along Dovetail Board from In-Plane Lateral Load Test

Figure 4-3: Elongation of Hole at the Bottom of Wall in In-Plane Lateral Load Test

4.2 Out-of-Plane Loading Test Results

The out-of-plane measured response of the wall is shown in Figure 4-4. The deflection used in Figure 4-4 is the deflection measured by hydraulic actuator. The out-of-plane loading test was designed to model a static load from wind or similar out-of-plane loading. The wall withstood a maximum load of 48 kips (213.5kN) and maximum midspan deflection of 3.3 inches (8.4cm) before failure. The wall began to fracture at approximately the same load of 48 kips (213.5kN) but at a midspan deflection of 2.5 inches (6.35cm). The wall then continued to sustained a load of at least 40 kips (177.9kN) for 0.8 inches (2.03cm) of deflection before complete failure. The wall response demonstrates the out-of-plane ductile behavior of an ICLT panel. The wall fractured below where one of the line loads was applied; where the bending stress and shear stress is the highest. At the maximum loading the wall had a bending stress of 857.8 psi (5.9MPa) and a shear stress of 83.3 psi (574kPa). Calculations can be found in Appendix D.

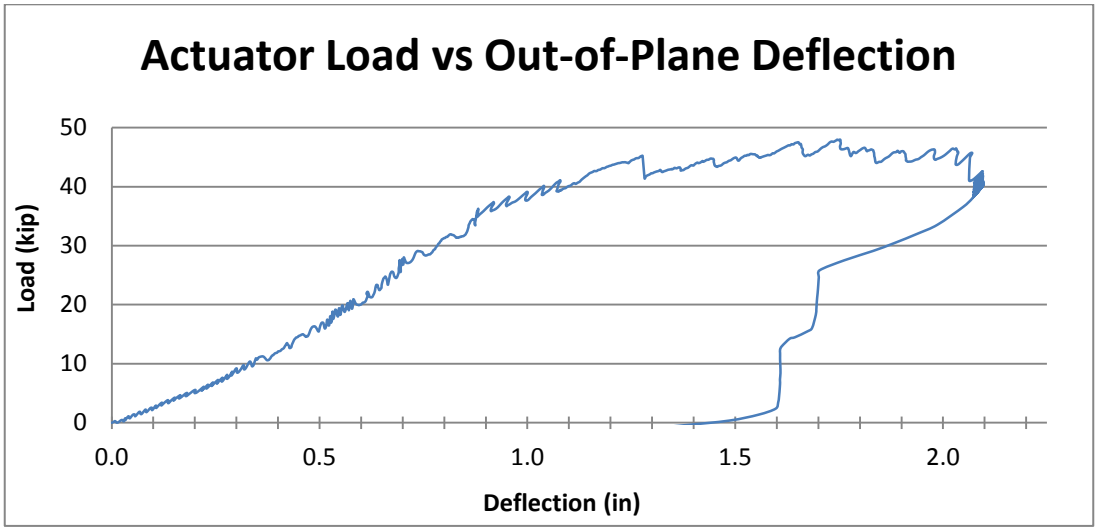

Figure 4-4: Actuator Load-Deflection Plot for the Out-of-Plane Loading Test

One of the interesting aspects of the configuration of the wall is the placement of dovetail boards in the wall. It appears that these dovetail boards acted as collectors for the system and helped distribute the load across the wall. However, due to both dovetail boards being adjacent to each other and the possible stress concentration at these boards where the outer layers have modified and reduced cross sectional areas, the wall may have actually have a “weak spot” at the locations of the dovetail boards. It was at such a location that the bottom board of the wall fractured in tension and the top boards split as shown in Figure 4-5.

Figure 4-5: Region of Failure at the Out-of-Plane Loading Test.

Due to the reduced cross section of the outer boards at the dovetail connections and the fact the interlocking dovetail boards were not spaced symmetrically in the wall, the wall most likely failed prematurely. If the dovetail boards had been spaced symmetrically in the wall and the reduced cross section of the outer members not been at the point of loading, the wall would

probably have a higher capacity. For this higher capacity scenario to occur, most likely all the outer dovetail pieces connecting to the inner layers should be placed symmetrically in the middle of the span, thus placing the outer members with the largest cross sectional area in the regions of higher bending moments. The reduced cross section outer members should be placed in regions closest to zero bending moment as much as possible. The orientation of the inner dovetail pieces connecting with opposite outer layers should not be placed adjacent to each other as shown in Figure 4-5. Additional figures and load-deflections curves corresponding to the out-of-plane loading test are found in Appendix B.

4.3 **In-Plane Vertical Load Test Results**

The axial loading test proved that the ICLT wall has a very high compressive strength. The wall sustained a maximum compressive load of 601 kips (2673kN) at a vertical deflection of 0.23 inches (5.8mm). This maximum load equates to 736 psi (5.08MPa) over the entire top of wall surface (see Appendix D for calculation). However, since the compressive strength almost entirely comes from the vertical members the stress can essentially be increased to 1192 psi (8.2MPa) assuming that only the outer layers resisted the load (see Appendix D for calculation). Due to the configuration of the wall the horizontal members of the wall resist little to none of the compressive load. The horizontal dovetail members simply act as lateral bracing for the vertical members. The wall failed at a maximum load of 601 kips (2673kN) as seven boards buckled at the top of the walls south face. Figure 4-6 shows the wall at fracture. Even after these boards buckled the wall maintained a 525 kip (2335kN) load for a significant period of time until the load was removed from the hydraulic jack.

Figure 4-6: Fracture of the In-Plane Vertical Load Test

Upon further evaluation of the wall as it was dismantled, the dovetail board that ran horizontal to the fractured members had its dovetail portion ripped completely off as shown in Figure 4-7. The internal lateral force the outer boards placed on the inner dovetail piece must have overcome the tension perpendicular to the grain strength of the wood. As the dovetail board fractured it increased the unbraced length of the outer layer boards thus reducing the compressive strength of the wall and causing the outer boards on the south face to buckle. Several of the buckled boards were completely fractured.

From the measured data shown in Figure 4-8 it was noticed that the wall began to bow toward the south until the 50 kip (222kN) load. At this load, the wall bowed to the north and would continue moving in that direction until failure, although at 550 kips (2446kN) the magnitude of bowing to the north decreased on average 0.15 inches (3.8mm) over the last 51

kips (226.8kN). Most likely due to this bowing action, some eccentricity was introduced into the system. In addition, the loading frame did move slightly toward the restraining channel on the north side of the reaction frame. This channel was designed to reduce the lateral movement of the beam. As the wall moved to the north, the distance between the bottom of the beam and the top of the south side of the wall decreased slightly while the distance between the bottom of the beam and the top of the north side of the wall increased slightly. These movements caused the south side of the wall to most likely resist more of the applied load, leading to the eventual failure of the south side of the wall. A schematic drawing of this possible scenario is shown in Figure 4-9. Additional figures and load-deflections curves corresponding to the in-plane vertical load test are found in Appendix C.

Figure 4-7: Fracture of Horizontal Dovetail Member, In-Plane Vertical Loading Test

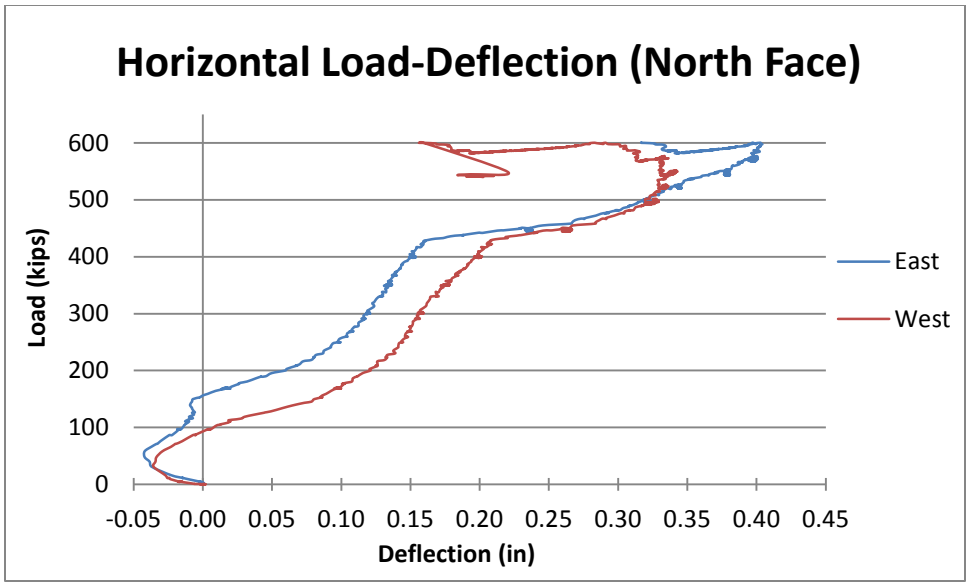

Figure 4-8: Horizontal Load-Deflection Curve for In-Plane Vertical Load Test

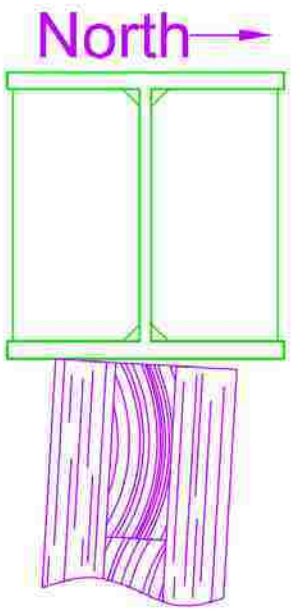

Figure 4-9: Movement of the Top of the Wall Relative to the Beam

5 MATERIAL PROPERTIES OF BEETLE KILLED TIMBER

This chapter is a synopsis of the material property findings from performing small clear wood tests on the beetle killed wood from the three-ply wall panels. The small clear wood tests were performed in order to determine beetle killed blue stained wood material properties. The hypothesis is that in order to develop a more accurate analytical model for ICLT panels it is necessary to know the material properties of the beetle killed wood. By knowing the material properties of the beetle killed wood one can also determine if they are similar to those of non-beetle killed wood of the same species. If these material properties were found to be similar then readily available reference design values in the NDS can be used for the analytical models and future ICLT design purposes. The material property tests were conducted by Uyema (Uyema 2012) and the author.

5.1 Beetle Killed Timber

As described in section 2.2 there are several effects of MPB attack on pine trees. Beetle boring holes, blue stain discoloration of the sap wood and the death of the tree are all effects of these attacks. Due to these effects beetle killed wood has traditionally not been used for stick framing or heavy timber construction. Recent studies have shown, however, that there is little to no significant difference in the material properties of blue stained beetle killed wood and normal grade lumber (Forintek, 2003). In Colorado, the New Town Builders construction company has

recently started to use the beetled killed wood for vertical stick framing in their projects but all lateral bracing is still done with normal graded lumber (Svaldi, 2011).

The research performed by Uyema (Uyema 2012) and the author was a collection of tests similar to those Forintek performed (Forintek 2003). Tests conducted were static bending, compression parallel and perpendicular to the grain, shear parallel to the grain, and tension parallel and perpendicular to the grain. The tests were conducted according to ASTM D143-09 - Standard test methods for small clear specimens of timber. A full report of these tests can be found in Uyema (Uyema 2012). Presented herein is a summary and brief discussion of the relevance of these tests to ICLT panels.

5.2 **Material Property Results**

The results from the performed tests for all cases except static bending were conclusive that there is no significant difference in the material properties of non-MPB killed wood and those of MPB-killed (Uyema 2012). For the case of static bending, results were well below that of adjusted NDS design values. This may be due to the fact the secondary method from ASTM D143-09 was used during testing. The secondary method does obtain smaller values than the primary method (Materials 2010). Also there is no specified sample size for the test and had a larger sample size been used during the testing by Uyema, most likely the results would have been closer to NDS design values.

Due to the variableness of wood strengths a 5% exclusion value is used as a starting point for development of reference design values (Breyer 2007). This means that 95% of all clear samples tested for a particular species would be expected to have strength at or above the

reference design value. Table 5-1 summarizes the results of the small clear wood tests along with associated NDS values.

Table 5-1: NDS Adjusted Design Values vs. Test Results (Uyema, 2012)

	NDS Adjusted Design Values (psi)			Test Results (psi)		
	No. 2	No. 3	Stud	Min	Average	Max
Static Bending	1674	972	1296	456	699	845
Compression Parallel	2484	1428	1418	3985	6251	8714
Compression Perpendicular	447	447	447	523	975	1497
Tension Perpendicular	290-350*			176	300	471
Tension Parallel	1134	648	653	1263	2990	4669
Shear Parallel	292	292	292	856	1055	1569

* Range of tensile strength created from values of Lodgepole pine and Engelmann spruce from the Wood Handbook

As shown in Table 5-1 all the recorded test results are well above the 5% exclusion value used to determine the NDS design values. In light of these results, adjusted reference design values will be used in the developed analytical models. Results will then be compared to the actual measured results of the ICLT panel tests.

To determine the ICLT wall panel strengths the NDS values for bending, compression perpendicular to the grain and compression parallel to the grain of the wood category Spruce-Pine-Fir South which includes Lodgepole Pine, which is the predominate species the ICLT walls were built from, will be used. The tension perpendicular to the grain value of 290 psi (1.99MPa) for Lodgepole pine from the wood handbook will also be used for calculations (FPL 2010). The tension perpendicular to the grain value from the wood handbook is used because the NDS does not have a design value for tension perpendicular to the grain since this is the weakest orientation of wood and is to be avoided. The design calculations will be based on the observed mode of

failure for each wall, taking the orientation of where the walls failed into consideration. The calculated values and measured results as well as comparison and discussion of the findings are presented in Chapter 6.

6 ANALYTICAL MODELS FOR ICLT PANELS

Analytical models were developed for strength predictions after the tests were completed on the three wall panels. The calculations for the models were based on the conclusions that blue stained beetle killed timber does not have a significant reduction in strength, thus NDS design values from the timber category Spruce-Pine-Fir South (Council 2005) and the strength value for tension perpendicular to the grain from the Wood Handbook (FPL 2010) were used.

6.1 Analytical Models

The three analytical models developed in this text were based on the orientation of the ICLT panels and how the individual layers in the panels interacted as an entire panel system. The interaction between layers and the mode of failure of the panels were expressed in the simplified analytical models discussed in this section.

6.1.1 Racking Strength Analytical Model

The in-plane lateral load test was performed to measure the racking strength on an ICLT panel. When the wall was disassembled the only evidence of failure were crushing marks perpendicular to the grain on all the dovetail boards. These marks were caused from the interaction of the vertical members interlocking with horizontal dovetail members and vice versa. When the top of the panel was displaced along the length of the wall the vertical boards

were put on a skew while the horizontal members remained relatively level. The rotation of the vertical boards caused a “binding connection” as shown in Figure 6-1.

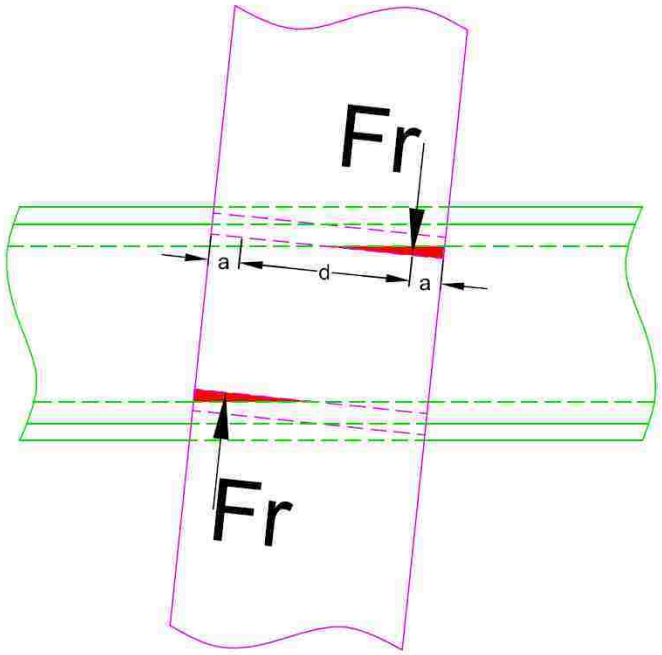

Figure 6-1: Binding Connection of Members in In-Plane Lateral Load Test

As the members became bound up, a crushing force was applied to the dovetail section of the horizontal board by the edges of the displaced vertical board. The force also caused a crushing force to be applied to the vertical board, but such crushing occurred parallel to the grain. Thus the weak “link” is the crushing perpendicular to the grain on the horizontal board. These two crushing forces, as shown in Figure 6-1 cause a small coupled moment on the dovetail section of the horizontal board. Equilibrium requires that the dovetail applies an equal and opposite moment on the opposing vertical board.

The analytical model for the racking strength was developed by examining an individual vertical member of the racking wall. The board is modeled as pinned-pinned with a shear force on top and reaction forces on the bottom of the board. The interaction of the horizontal dovetail members on the vertical member are applied as moments. A schematic drawing of this model is shown in Figure 6-2.

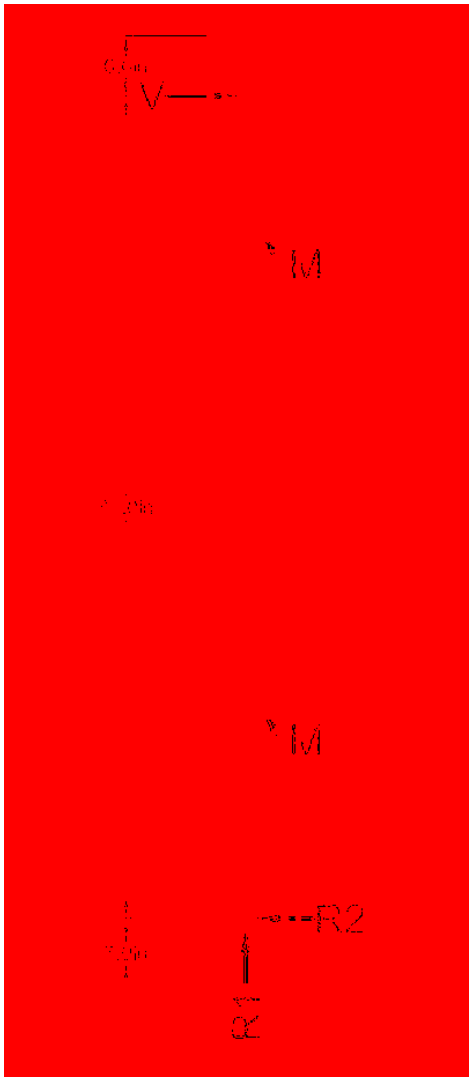

Figure 6-2: Analytical Model for Racking Strength of ICLT Panel

As the shear force increases on the vertical board the moments must increase as well to maintain equilibrium. The wall panel used for the in-plane lateral load tests had 22 vertical members (11 on each outer layer) that interacted with the horizontal dovetail members as shown in Figure 6.2. The wall panel also had four vertical dovetail members (two on each outer layer) that interacted with all 13 horizontal members (wall middle layer). These four vertical members can be modeled just like the other 22 vertical members except instead of just two moments being applied to the vertical member there are 13 moments applied to the vertical member. Once the shear force is calculated for the two different types of vertical members the total racking force on the ICLT panel can be approximated by adding up all the shear forces of the individual vertical members.

6.1.2 Flexural Strength Analytical Model

The out-of-plane loading test was set up as a simply supported beam with two equal line loads spaced at third points along the span. The outer layers were the “active bending layers” with the line load orientated perpendicular to the boards on these active bending layers while the middle layer was orientated parallel with the line loads and resisted little to none of the load and acted only to help evenly spread the load to the active bending layers. The analytical model developed to predict the flexural design load for the wall was based on the ratio of the moments of inertia of the active boards to an idealized solid wall. The moment of inertia for the ICLT wall panel was calculated as the outer layers of the wall separated by a “void” that was composed of the middle layer and the inner inch (2.54cm) of material from the dovetail cut on the outer layer boards. The inner 1.0 inch (2.54cm) of material is removed to better represent the weakest parts of the outer boards, where the dovetail from the middle section interlocks with the outer boards.

This orientation can be seen in Figure 6-1. The material outside of the dotted lines is considered effective while the region enclosed by the dotted lines is considered void. The ratio of the two moments of inertia is used to reduce the calculated capacity of the solid wood wall.

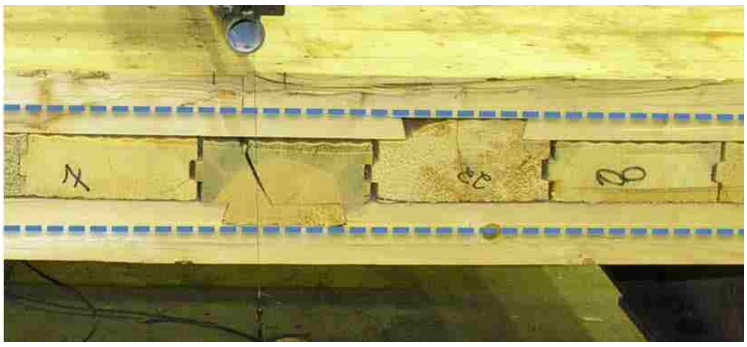

Figure 6-3: Division for ICLT Flexural Design Strength

6.1.3 Compressive Strength Analytical Model

The analytical model for the in-plane vertical load test was simplified to be the design of a continuous wood column with a pinned connection at each of the horizontal dovetail locations. By using the longest vertical unbraced length of a board to calculate the buckling capacity of that board and then multiplying that strength by the number of vertical members, an approximate compressive strength of an ICLT panel is obtained. The vertical boards in a panel act as lateral support in the strong axis for each adjacent board (i.e., an individual vertical board cannot buckle about its strong axis) and the middle horizontal dovetail members acted as lateral support in the weak axis. An individual vertical board can buckle about its weak axis. Essentially the unbraced length for a vertical board is the greatest distance between two horizontal dovetail members. For the ICLT wall panel the unbraced length of a vertical board is 48 inches (1.22m). The average

full sized board with cross sectional dimensions of 2.625 x 7.5 inches (6.7cm x 19cm) was used as the design wood column.

The continuous vertical board was modeled as a 48 inch (1.22m) piece representing the middle section of the board (length of 48 inch (1.22m)) and another piece at the top and bottom representing the two smaller 24 inch (61cm) sections. Since the top and bottom of the vertical board are simply supported these 24 inch (61cm) sections were lengthened to 48 inches (1.22m) in order to model the full action of a beam in a space frame. Using a sidesway inhibited alignment chart the "K" factor for the middle 48 inch (1.22m) board was calculated to be 0.55.

The two vertical dovetail boards interlock with all the horizontal boards and are continuously supported in the weak and strong axis. This would allow the vertical dovetail boards to have a higher compressive capacity. Despite having a higher capacity and in lieu of the fact the panel still failed even though the vertical dovetail members did not buckle, for calculation purposes the vertical dovetail boards will be assumed to be simply vertical boards that are not continuously supported in the weak axis.

Along with the compressive strength of the wall a secondary calculation based on the tension perpendicular to the grain strength of the actual dovetail section was performed. This estimates the lateral force the vertical boards applied on the horizontal dovetail board when eccentricity is introduced to the system. The motivation for this secondary calculation is the fact that the horizontal dovetail board failed in tension perpendicular to the grain as shown in Figure 4-7.

6.2 Analytical Model Results

The results of the three analytical models described above were compared to the measured racking, flexural, and axial compression strengths of the wall respectively. A complete set of calculations are presented in Appendix D. All three models produced relatively accurate results for the ICLT panel strengths based on how each wall failed.

6.2.1 Racking Strength Analytical Model Results

The crushing forces from the interlocking of the vertical member on the horizontal dovetail cause a moment on the horizontal dovetail member as shown in Figure 6-1. This moment on the horizontal dovetail member applies an equal and opposite reaction moment on the vertical member. The crushing forces are calculated by assuming a triangularly distributed load applied to the dovetail section of the horizontal member. The area the crushing force is applied to is simplified to be half the width of the vertical board times the depth of the dovetail cutout. The calculations for the racking strength analytical model can be found in Appendix D under the section titled "Calculations for Racking Strength Analytical Model." For this particular racking wall the crushing area (A_c) was calculated to be 3.75 in^2 (24.2cm^2). The NDS adjusted design value for compression perpendicular to the grain (F_{cp}) is then calculated. The resultant crushing force (F_r) is expressed in equation 6-1.

$$\boldsymbol{F_r = \frac{1}{2} A_c F_{cp}} \quad \textbf{(6-1)}$$

Once the resultant crushing force is calculated the moment applied by the horizontal dovetail onto the vertical member can be determined. In Figure 6-1 the dimension "a" is the distance from the edge of the vertical member to the centroid of the triangularly distributed load of the crushing force. This is the location where the force F_r acts. The moment arm is the in-line

distance between the parallel forces F_r, or dimension “b” in Figure 6-1. The moment (M) is equal to the dimension “b” multiplied by F_r.

Once the moment applied to the vertical members from the interaction of the horizontal member is calculated the shear force applied to the vertical member is equal to the sum of the moments about the pinned connection at the bottom of the vertical board. Equation 6-2 is the expression of the calculated shear force where “n” is the number of moments applied to the vertical member and “h” is equal to the distance between the top and bottom of the wall.

$$\boldsymbol{V = nM/h} \quad \textbf{(6-2)}$$

The sum of all the shear forces applied to the vertical members is equal to the racking strength of the ICLT panel. Using an NDS compression perpendicular to the grain strength of 414 psi (2.85MPa) and following the racking strength analytical model, the shear force on a vertical member with just two applied moment was 93.7 pounds (416.8N) and a vertical dovetail member with 13 applied moments had an applied shear force 608.8 pounds (2.71kN). The calculated racking strength was 4.5 kips (20.02kN) at yield compared to the measured racking strength of 6 kips (26.7kN) at yield.

The difference between the calculated and measured yield strengths is most likely due to a secondary in-plane lateral resistance effect. One of the possible effects is the friction forces between layers and the tongue and groove connections between boards. The model developed does not account for the friction between vertical boards or the friction between horizontal boards.

6.2.2 Flexural Strength Analytical Model Results

The analytical model used for flexural strength predictions as explained in section 6.1.2 gives a strength value slightly higher than what was measured. The expected load was calculated from equation 6-2 where $F`_b$ is the bending stress of the wood beam, S is the beam section modulus and L is the span length of the beam.

$$P = \frac{6F`_bS}{L} \tag{6-3}$$

Equation 6-3 is a rewrite of the moment equation for a simply supported beam with two equal point loads at 3rd points and that stress times the section modulus is equivalent to the bending moment of a simply supported beam. The bending stress was calculated using the NDS adjustment values for design. For a step by step procedure of calculations see section titled "Calculations for Flexural Strength Analytical Model" in Appendix D. The design load for a solid simply supported wood beam is 83.5 kips (371.4kN). The ratio of the two small beams separated by a middle void model to the solid beam model was calculated to be 0.729. The predicted flexural strength of the wall panel was calculated to be 60.8 kips (270.4kN). This capacity is slightly higher than the measured capacity of 48 kips (213.5kN) for the wall. One possible reason for this decrease in capacity may be largely due to the orientation of the dovetail boards. By having the two middle dovetail boards side by side, the cross sectional area of the outer members is greatly reduced in a single section of the wall. Increased internal forces are also applied to the outer layers of the wall panels as the two dovetail boards try to rotate toward the outer layers due to the top of the wall being in compression and the bottom of the wall in tension.

6.2.3 Compressive Strength Analytical Model Results

The analytical model used for compressive strength predictions for the ICLT panel made the assumption that each vertical member was a continuous column with a pinned connection at each horizontal dovetail, each vertical member laterally supported the adjacent vertical member in the strong axis, and the horizontal dovetail members laterally supported the vertical members in the weak axis. Using the NDS adjustment factors the compressive strength for a single vertical member of the wall with an unbraced length of 48 inches (1.22m) is 1435.4 psi (9.89MPa). By simply multiplying the compressive strength by the total cross sectional area of the vertical members in the wall, a total compressive strength of 734.8 kips (3.27MN) is predicted. This is greater than the actual measured compressive strength of 601 kips (2673kN).

The difference between the measured and calculated strength is most likely due to the eccentricity that occurred during testing. As discussed in section 4.3 the load was applied at a higher concentration on the south side of the wall due to the top beam rotating to the south relative to the wall. From Figure 4-6 it is also notable the vertical members in the middle of the south face buckled while the outer three vertical members on each side didn't buckle. This shows that the load was more concentrated in the midspan of the wall then on the edges. Thus the load was more concentrated in the middle of the south side of the panel which is where the wall failed.

Part of the failure of this wall was also due to the horizontal dovetail nearest the top failing in tension perpendicular to the grain and suddenly increasing the unbraced length from 48 (1.22m) inches to 72 inches (1.83m). A calculation to predict the necessary internal lateral force on the outer layer boards on the south face of the wall was performed. Using the average tension perpendicular to the grain strength of 290 psi (1.99MPa) from the wood handbook and

multiplying it by the area of the dovetail section that failed, a force of 65.25 kips (290.2kN) was calculated. This internal force would have been introduced from the eccentricity of the vertical load on the wall creating secondary order effects. The tension perpendicular to the grain failure of the dovetail caused a premature failure of the wall. The model does not account for this behavior.

Table 6-2 summarizes all the calculated results and measured wall strengths for the three tests performed on the wall panels.

Table 6-1: Calculated and Measured Results of all Three Panel Tests

	Racking Strength at Yield	Flexural Strength	Axial Strength
Calculated (kip)	4.5	60.8	734.8
Measured (kip)	6	48	601

7 CONCLUSION AND RECOMMENDATIONS FOR FUTURE RESEARCH

Interlocking cross laminated timber wall panels are a building method that is implementing beetle killed wood in an interlocking layered configuration to build strong and sustainable wood structures. The three tests performed and discussed in this thesis show many of the structural benefits of ICLT panels. The panels are much stronger than conventional wood construction methods (Sanders 2011) and don't use expensive mechanical fasteners or toxic adhesives to connect individual pieces.

As part of this research, a set of simplified analytical models were developed. Although the racking model is slightly conservative while the flexural and axial models are slightly non-conservative, the simplified models are able to predict reasonably well the measured racking, flexural and compressive strengths of ICLT panels.

7.1 Additional Testing Recommendations

There are many additional tests needed to be performed before accurate engineering design methods can be established for ICLT panels. All three tests would need to be performed on three ply walls multiple times in order to increase the sample size. Testing five ply panels to determine if there is a correlation between the number of plies would also be necessary.

The in-plane lateral load tests would also need to be performed and then disassembled and evaluated at the drift limit state to determine how the wall as a whole is acting. Knowing

how many of “binding” points causing the resisting moments are engaged and when they are engaged needs additional testing. Additional displacement data is needed for movement of individual boards in order to determine if vertical members move independently or as an entire system. Load readings at binding points inside the wall would also be necessary in order to better understand the internal crushing failure of the wall panels.

The out-of-plane loading test would need to be performed on walls with different arrangements of the dovetail members within the wall and with respect to each other. This would determine if having dovetail boards not adjacent to each other would in fact increase the flexural strength of the panels. Testing with different loading types would also benefit understanding the overall flexural strength of the panels.

The in-plane vertical load tests would need to be performed to tighter tolerances in order to try to eliminate eccentricity and secondary order effects in the panels. Additional tests would also need to be performed on wall panels with window and door cut outs.

These tests and observations would help refine and validate the simplified set of models developed.

7.2 **Summary**

Interlocking Cross Laminated Timber (ICLT) wall panels are a new wood construction product. Besides being an innovative structural system, they also utilize beetle killed timber from many of the forests that have been devastated by the Mountain Pine Beetle. The in-plane lateral load, out-of-plane load, and in-plane vertical load tests performed on ICLT wall panel added to the previous structural tests performed on ICLT panels by Sanders (Sanders 2011) and show the strength and ductility of ICLT panels as a building material. The analytical models developed in

this thesis show promise in calculating the racking strength, flexural strength and axial compressive strength of ICLT panels. Additional tests and research are needed in order to refine the models before they can be used for structural design. Once these design methods are developed, ICLT wall panels have the potential to be another strong building material for all types of wood structures.

REFERENCES

AISC, A. I. o. S. C. (2005). "Steel Construction Manual." AISC, ed., American Institute of Steel Construction.

Apostol, K. (2011). "ICLT panel assembly." Heber City, UT.

Breyer, D. E., Frindley, K. J., Cobeen, K. E., and Pollock, D. G. (2007). *Design of Wood Structures ASD/LRFD*, McGraw-Hill.

Council, A. W. (2005). "National Design Specification for Wood Construction (NDS)." A. F. P. Association, ed., Washington, DC, 242.

Engineers, A. S. o. C. (2010). "Minimum design loads for buildings and other structures." A. S. o. C. Engineers, ed.

Forintek. (2003). "Properties of lumber with Beetle-Transmitted Bluestain." Wood Protection Bulletin, FPInnovations, ed., Forintek Western Division, 4.

FPInnovations. (2011). *Introduction to cross-laminated timber*, British Columbia, Canada.

FPL, F. P. L. (2010). "Wood Handbook, Wood as an Engineering Material." C. Edition, ed., U.S. Department of Agriculture, Forest Service, Madison, WI.

Knaebe, M. (2002). "Blue Stain." Techlines, Forest Products Laboratory.

Leatherman, D. A., Aguayo, I., and Mehall, T. M. (2007). "Mountain Pine Beetle." Trees and Shrubs.

Materials, A. S. f. T. a. (2010). "Standard Test Methods for Small Clear Specimens of Timber." ASTM D143-09, A. S. f. T. a. Materials, ed., Philadelphia, PA.

Sanders, S. (2011). "Behavior of Interlocking Cross-Laminated Timber Shear Walls," Project, Brigham Young University, Brigham Young University.

Smith, R. E. (2011). "Interlocking Cross-Laminated Timber: alternative use of waste wood in design and construction." BTES Conference 2011.

Structurlam. (2010). "Cross Laminated Timber Design Guide." CrossLam British Columbia, Canada, 10.

USDA. (2011). "Economic Use of Beetle-Killed Trees." F. P. L. Forest Service, ed., 10.

Uyema, M. (2012). "Effects of Mountain Pine Beetle on Mechanical Properties of Lodgepole Pine and Englemann Spruce," Masters Project, Brigham Young University, Brigham Young University.

Ward, R. (2009). "Going to New Heights, Building the World's Tallest Mixed-use Wood Structure." Structure Magazine, 3.

APPENDIX A. IN-PLANE LATTERAL LOADING TEST (RACKING WALL)

Additional figures of test setup, wall failure and graphs of in-plane lateral loading test.

Table A-1: Values from Racking Test Data

Average change in load (lbs)	9.52
Average drop > 100 lbs	191.03
Max load drop (lbs)	762.45
Max load Increase (lbs)	548.55
Average Diff in Actuator and SP16 (in)	0.6709
Max Diff in Actuator and SP16 (in)	1.1040
Max Diff under wall (in)	1.3423
Maximum Drift (in)	8.4552

Table A-2: Values from Racking Test Data, SI Units

Average change in load (N)	42.34
Average drop > 444.8N	849.70
Max load drop (N)	3391.38
Max load Increase (N)	2439.95
Average Diff in Actuator and SP16 (cm)	1.70
Max Diff in Actuator and SP16 (cm)	2.80
Max Diff under wall (cm)	3.41
Maximum Drift (cm)	21.48

Figure A-1: Top Connection of Racking Wall to Loading Frame

Figure A-2:Lateral Displacement of Racking Wall at Tests Limit

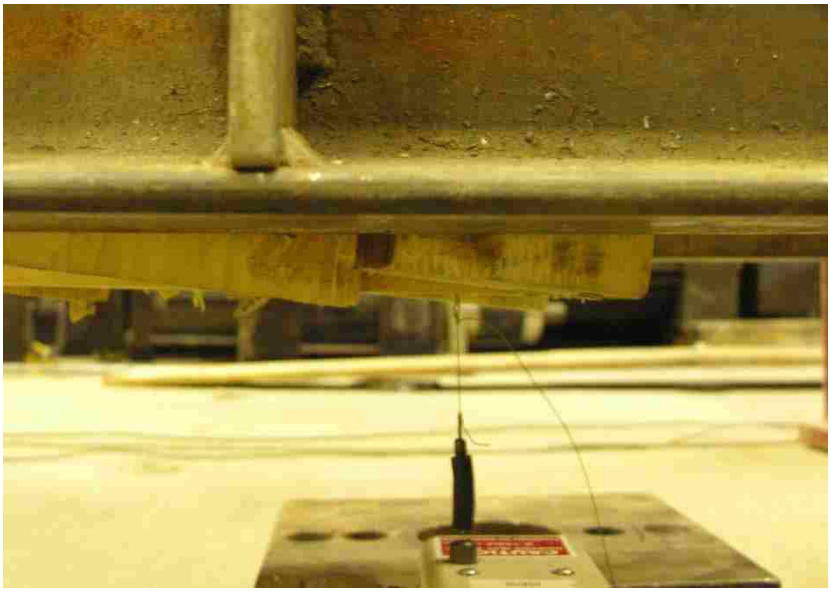

Figure A-3:Vertical Displacement of Racking Wall, East Side

Figure A-4:Vertical Displacement of Racking Wall, West Side

Figure A-5:Crushing of Dovetail Section in Racking Wall

Figure A-6:Measured Crushing of Dovetail Section in Racking Wall

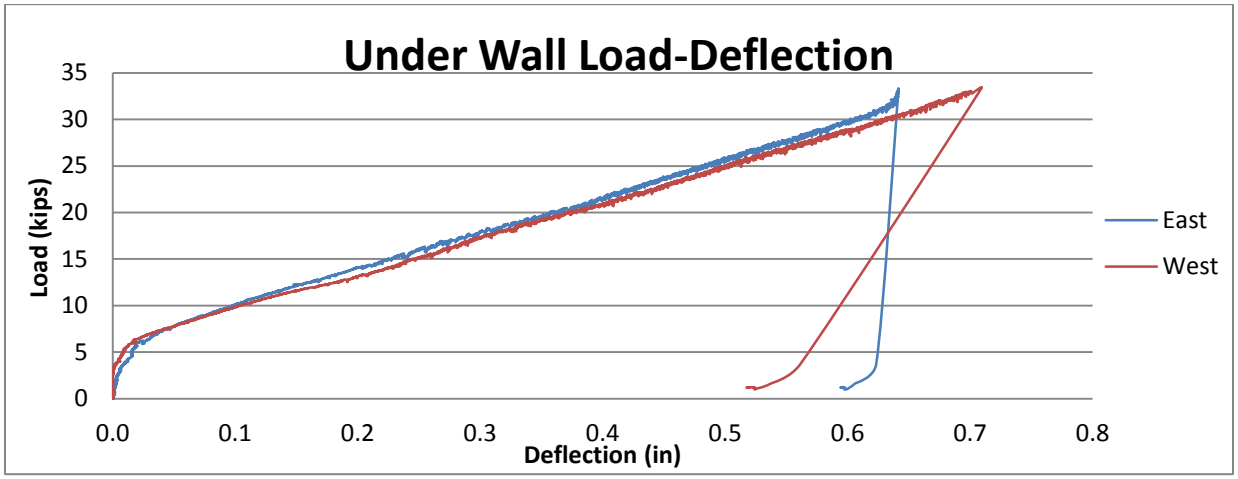

Figure A-7: Under Wall Load-Deflection Curve of Racking Wall

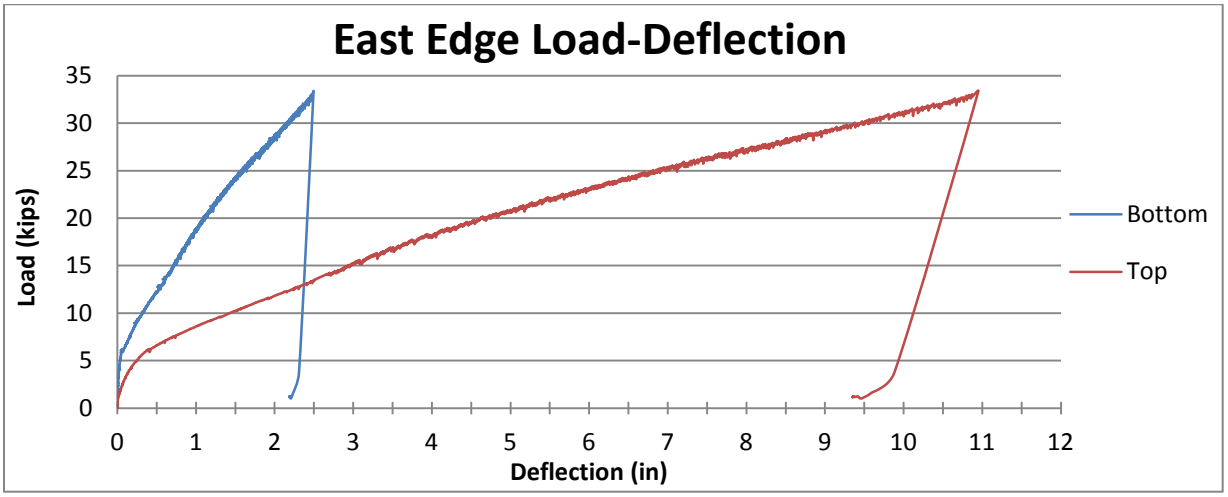

Figure A-8: East Edge Load-Deflection Curve of Racking Wall

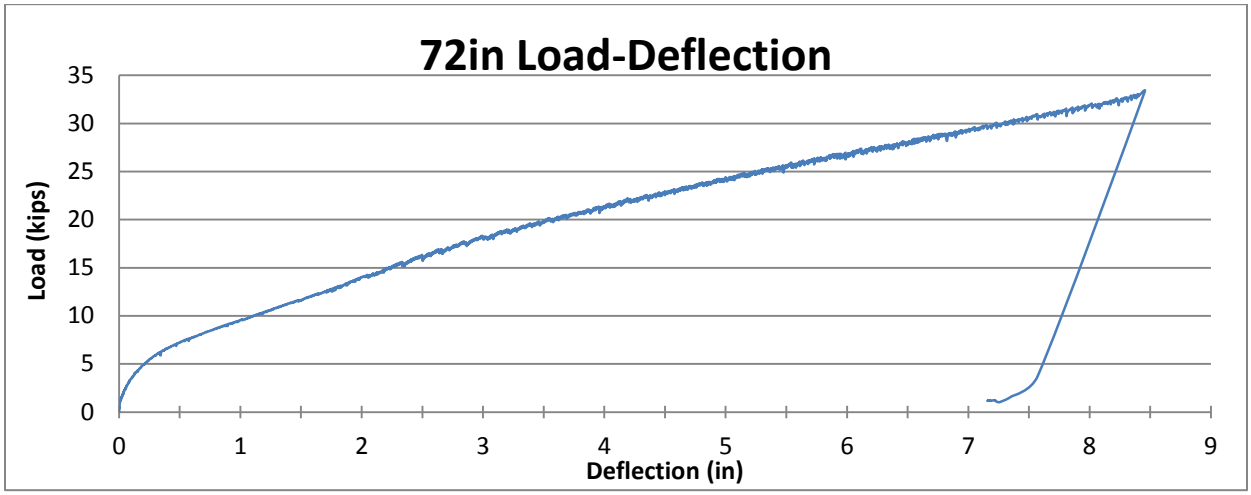

Figure A-9: Drift Load-Deflection Curve of Racking Wall

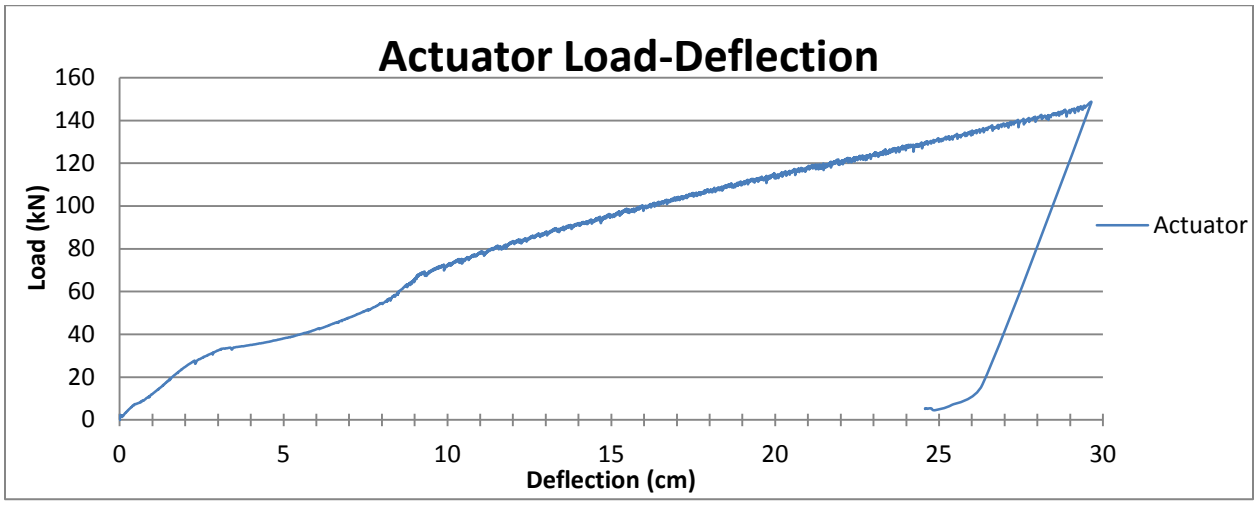

Figure A-10: Actuator Load-Deflection Curve of Racking Wall, SI Units

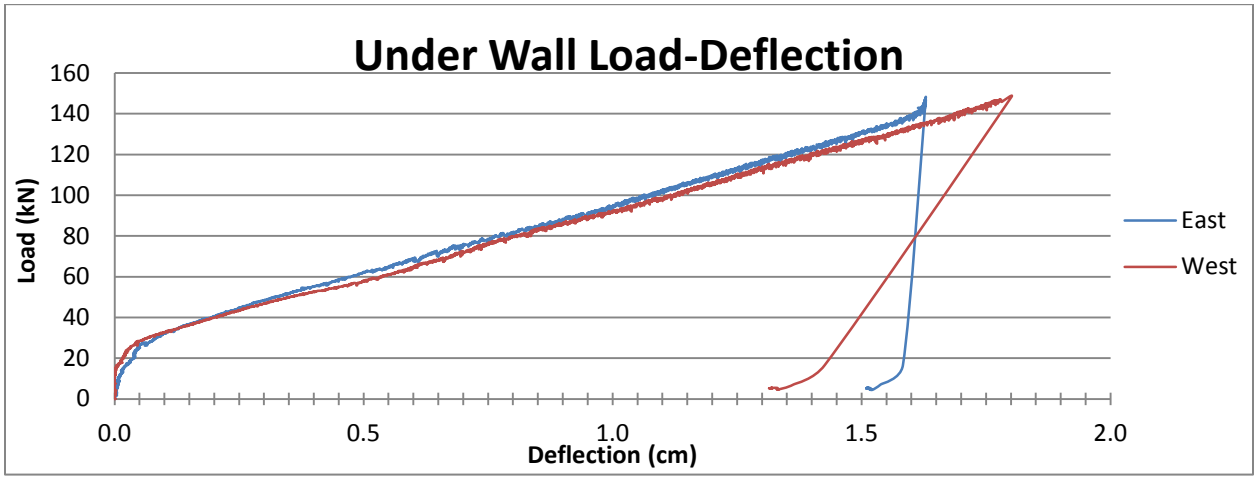

Figure A-11: Under Wall Load-Deflection Curve of Racking Wall, SI Units

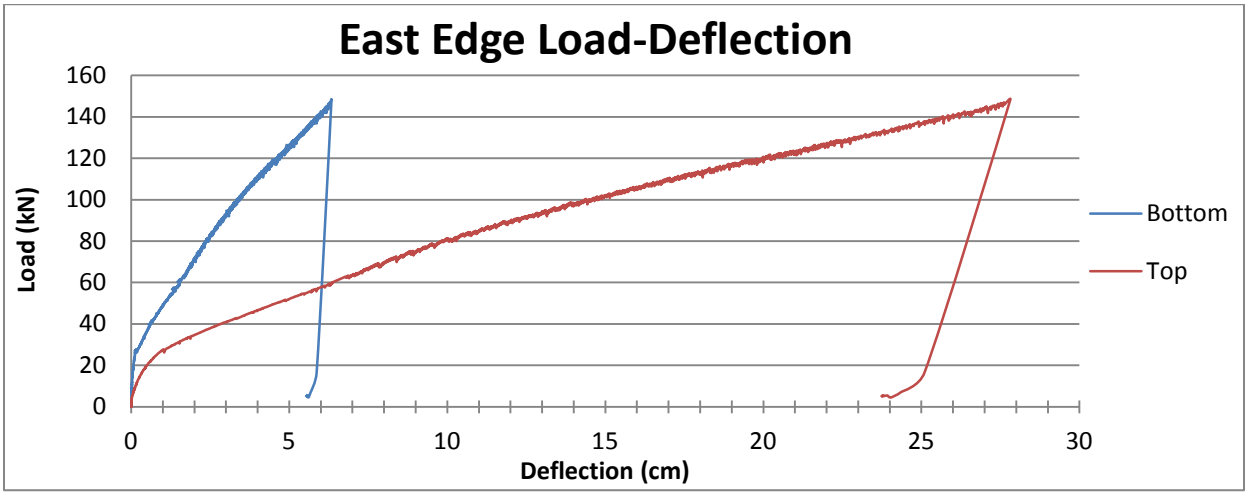

Figure A-12: East Edge Load-Deflection Curves of Racking Wall, SI Units

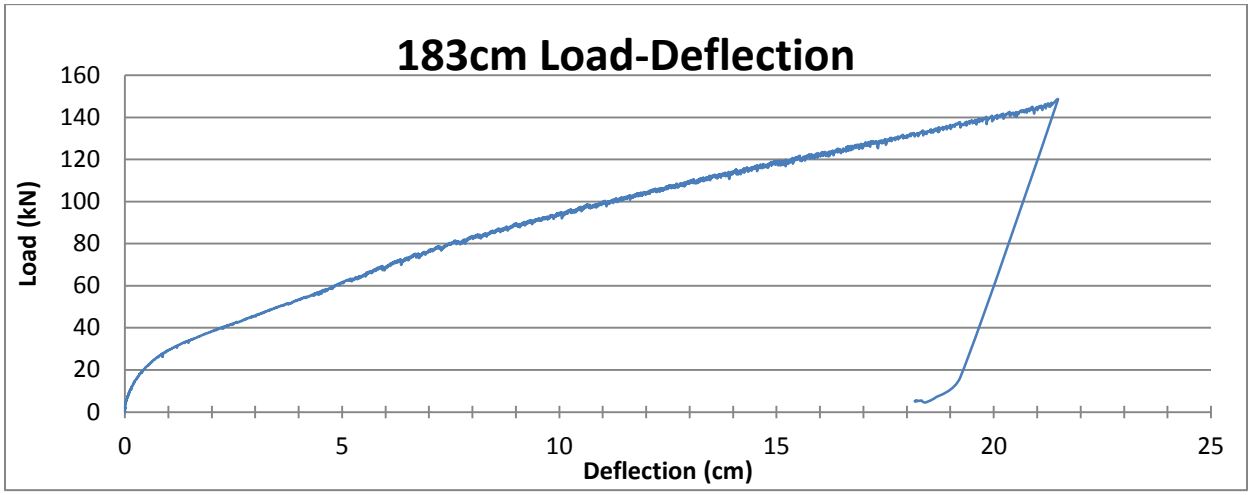

Figure A-13: Drift Load-Deflection Curve of Racking Wall, SI Units

APPENDIX B. OUT-OF-PLANE LOADING TEST (FLEXURAL WALL)

Additional figures of test setup, wall failure and graphs of out-of-plane loading test.

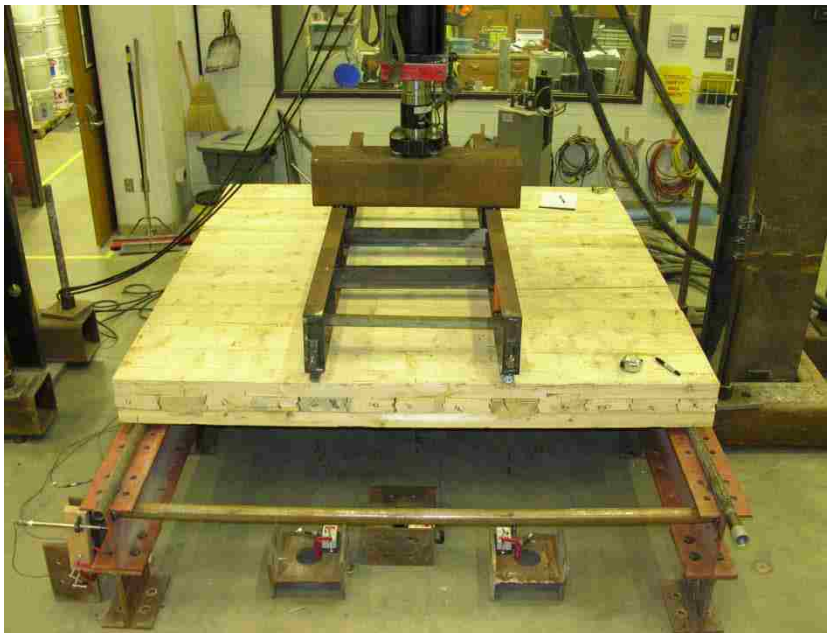

Figure B-1: Flexural Wall Test Setup Looking to the South

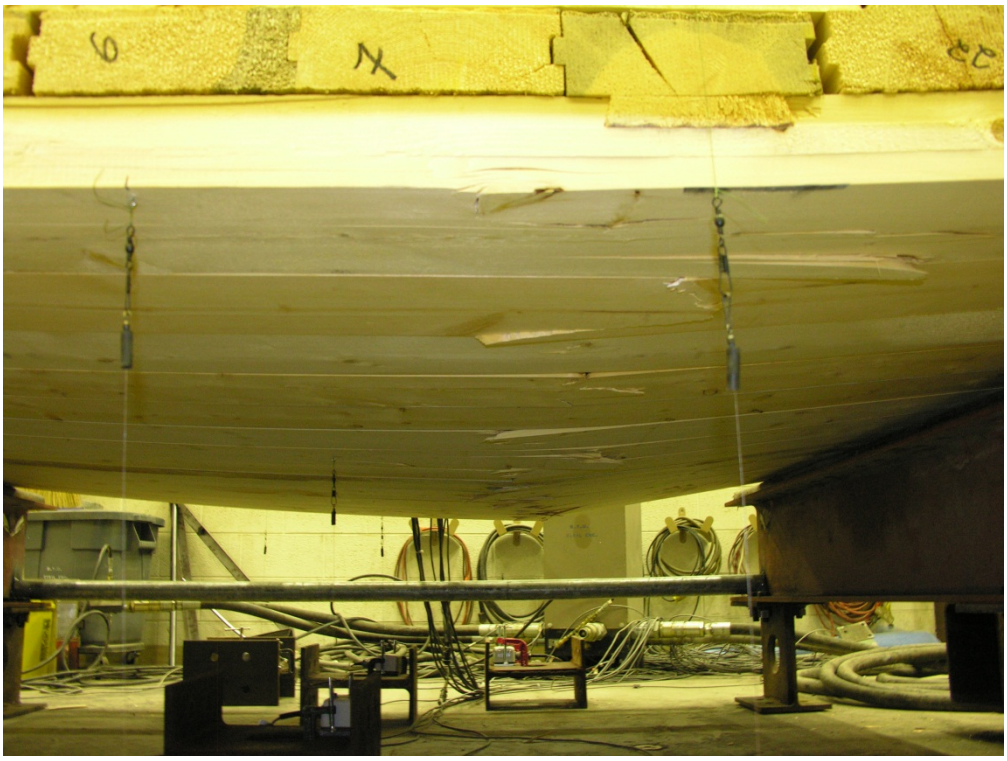

Figure B-2: Failure of Underside of Flexural Wall

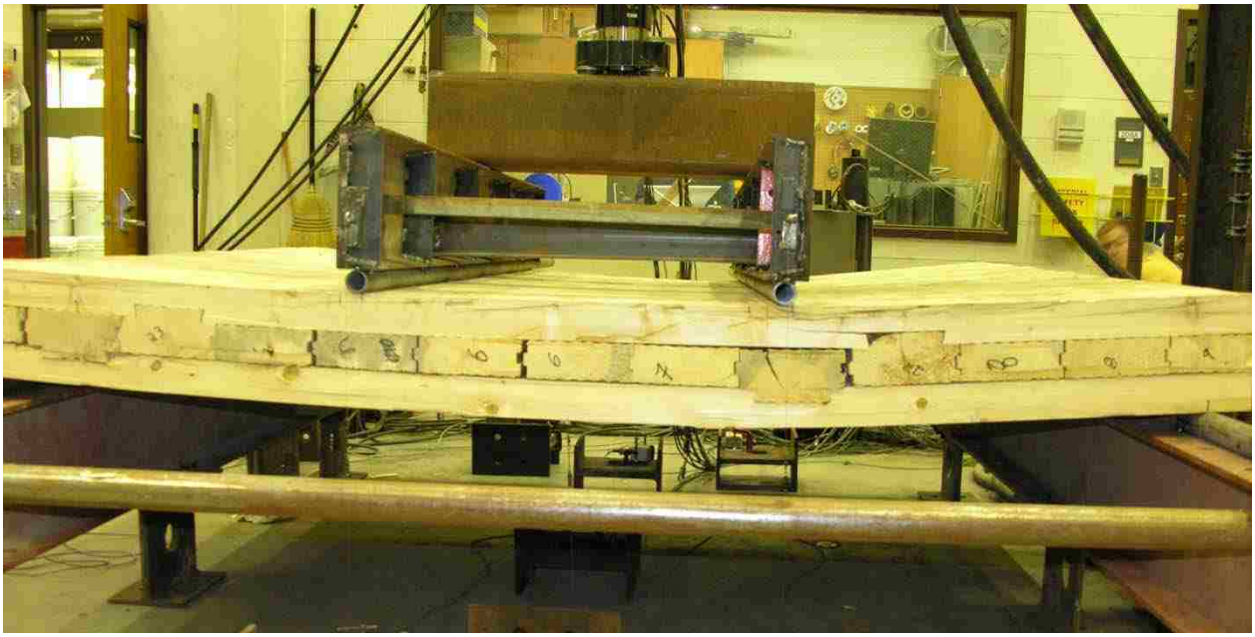

Figure B-3: Failure of Flexural Wall on the North Side

Figure B-4: Failure of Flexural Wall on the South Side

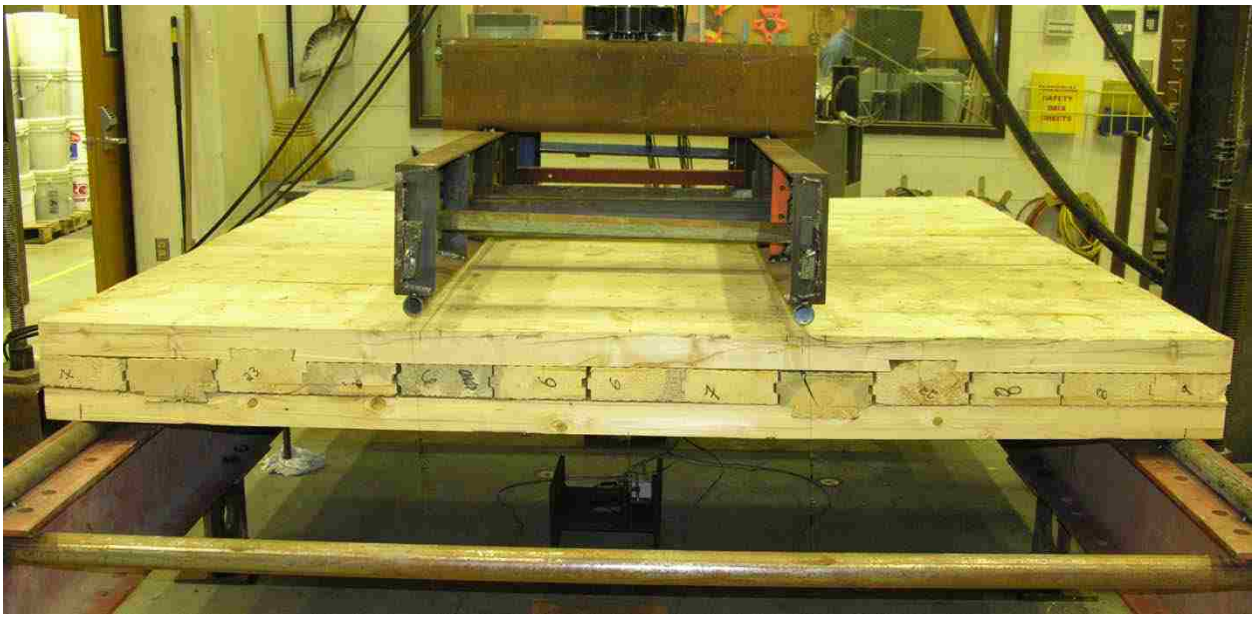

Figure B-5: Rebound of Flexural Wall after Failure on the North Side

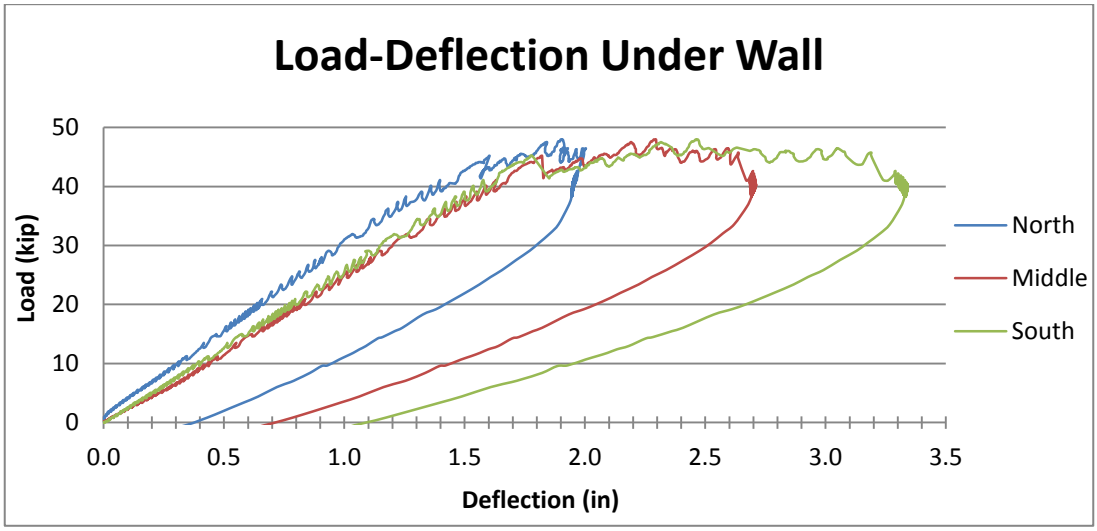

Figure B-6: Load-Deflection Curve of Underside of Flexural Wall

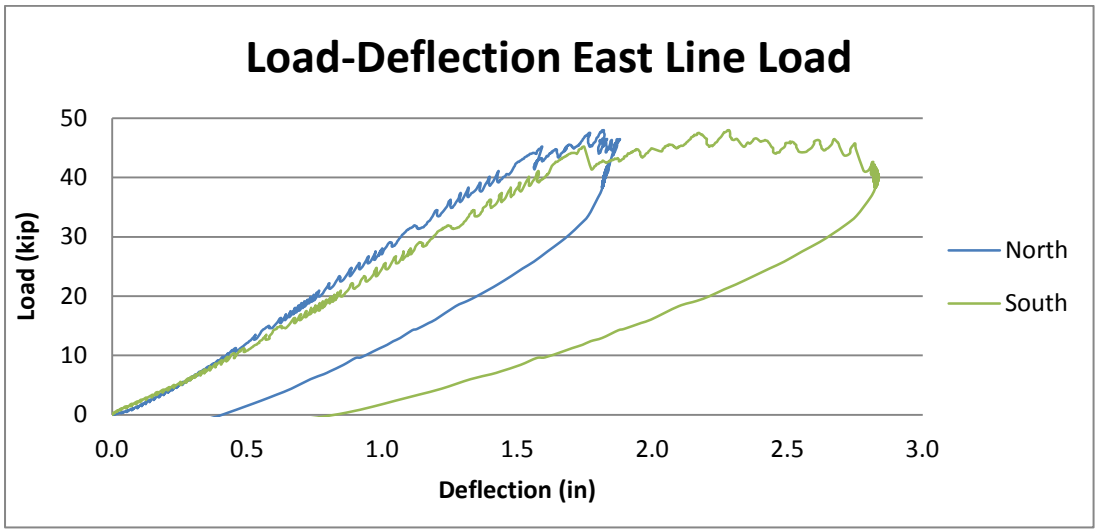

Figure B-7: Load-Deflection Curve of the East Line Load of Flexural Wall

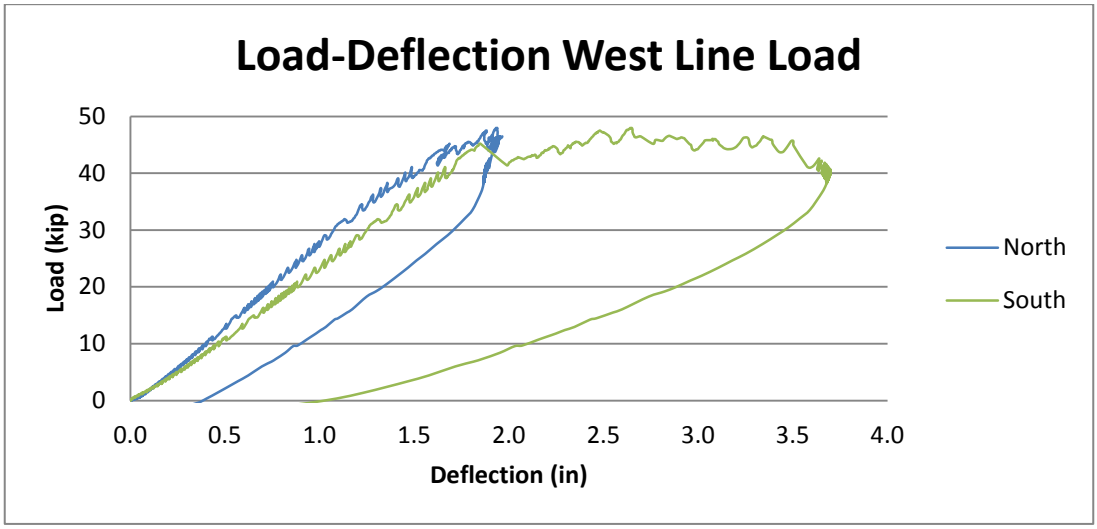

Figure B-8: Load-Deflection Curve of the West Line Load of Flexural Wall

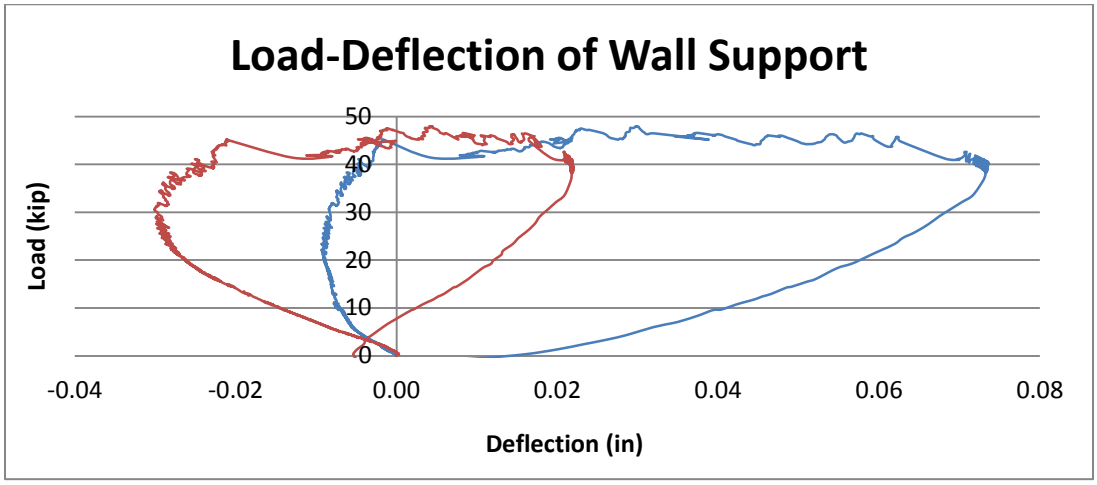

Figure B-9: Load-Deflection Curve of East Support Frame of Flexural Wall

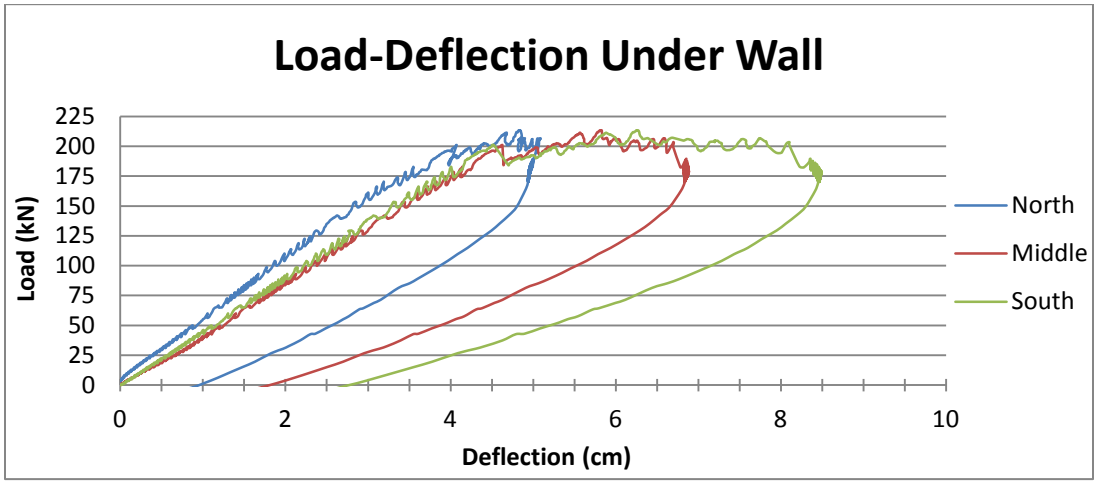

Figure B-10: Load-Deflection Curve of the Underside of Flexural Wall, SI Units

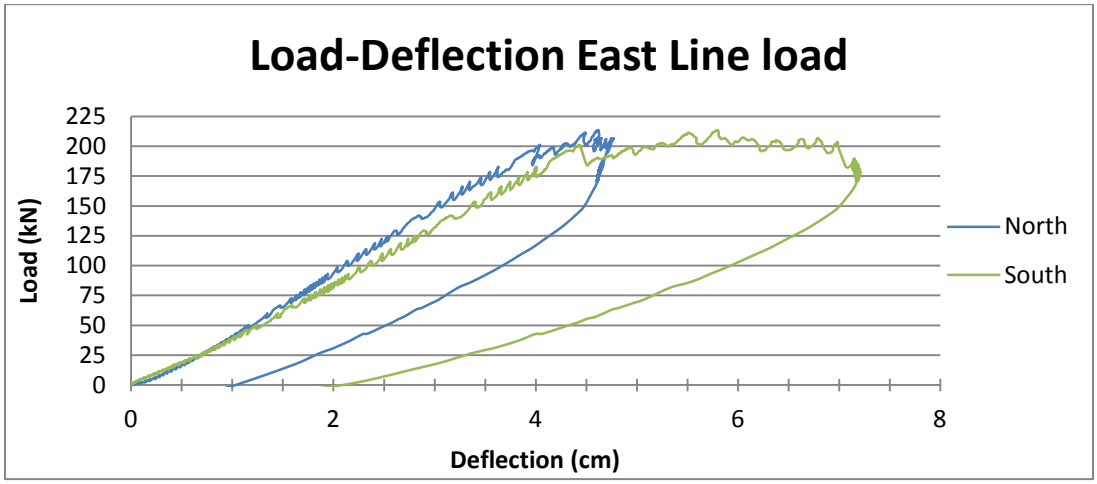

Figure B-11: Load-Deflection Curve of the East Line Load of Flexural Wall, SI Units

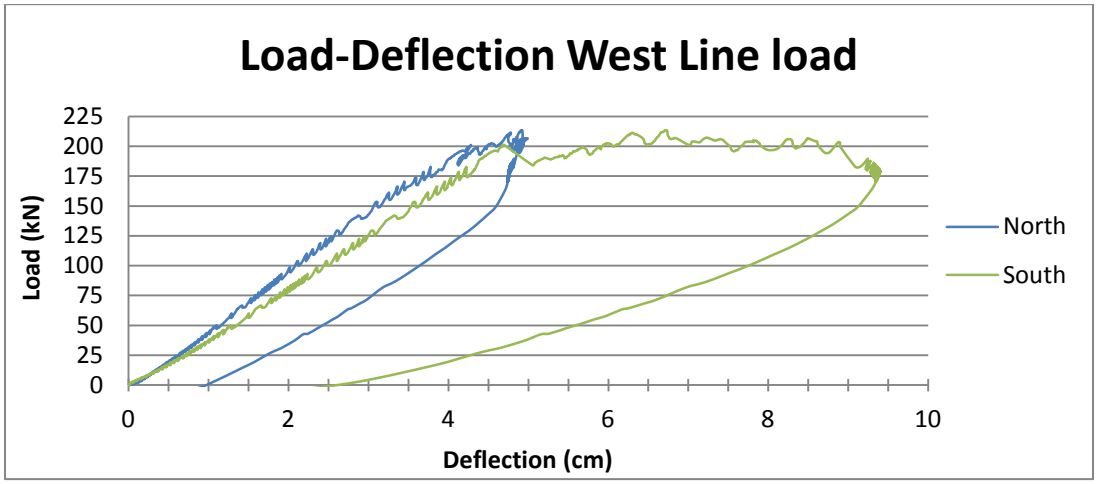

Figure B-12: Load-Deflection of the West Line Load of Flexural Wall, SI Units

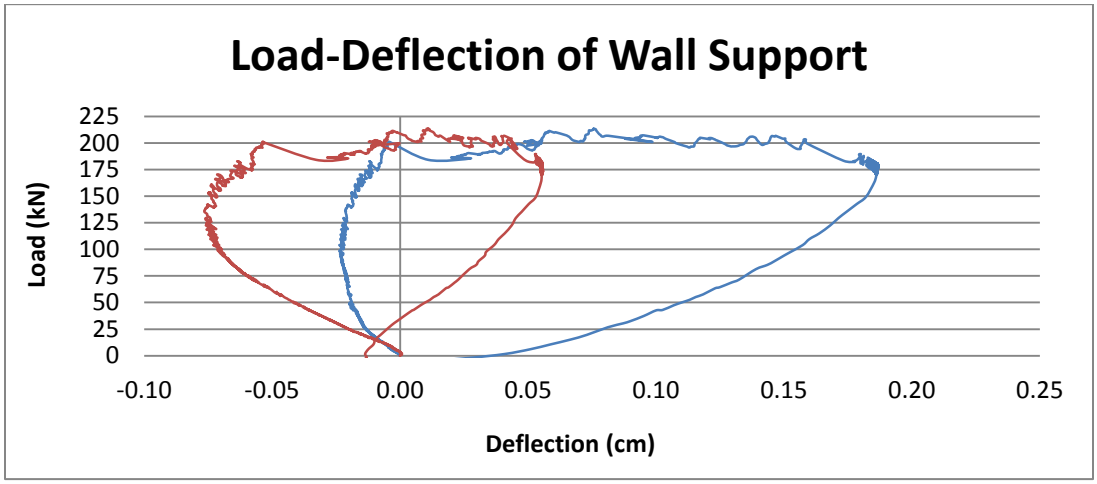

Figure B-13: Load-Deflection Curve of East Support Frame of Flexural Wall, SI Units

APPENDIX C. IN-PLANE VERTICAL LOADING TEST (AXIAL WALL)

Additional figures of test setup, wall failure and graphs of in-plane vertical loading test.

Figure C-1: North Face of Compression Wall Test Setup

Figure C-2: South Face of Compression Wall Test Setup

Figure C-3: Hydraulic Jack and Loading Frame of Compression Wall

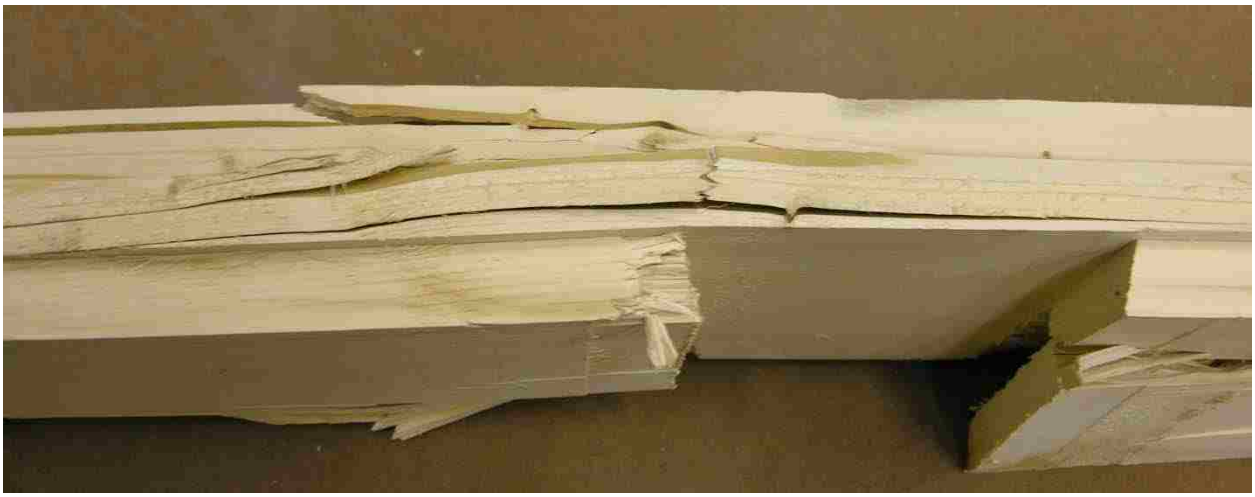

Figure C-4: Typical Buckling Failure of Vertical Members in Compression Wall

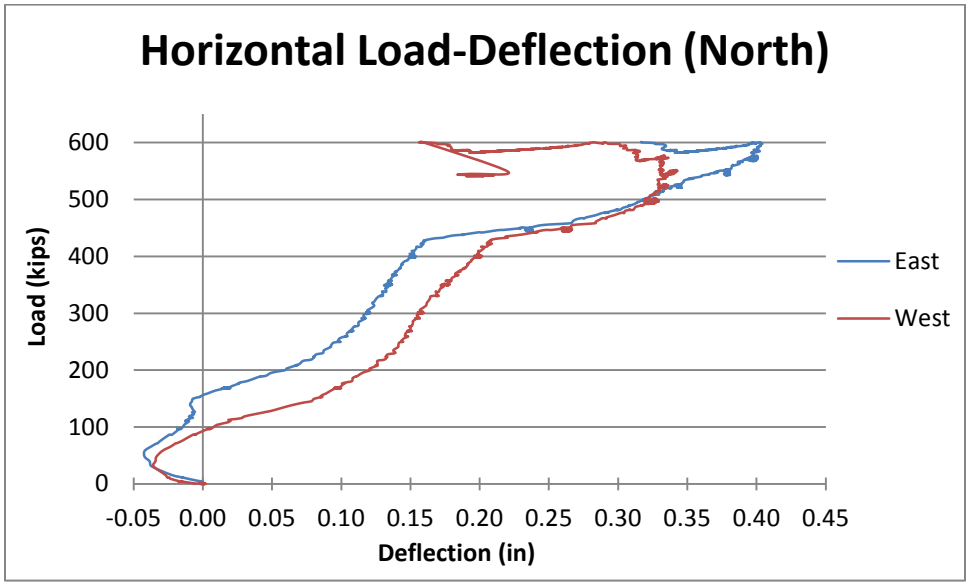

Figure C-5: Horizontal Load-Deflection Curve of Compression Wall, North Face

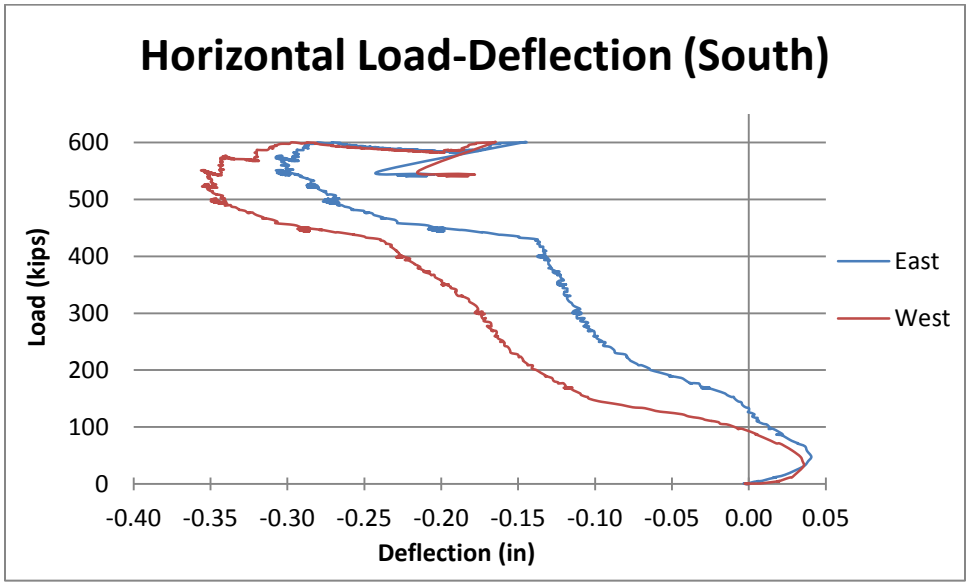

Figure C-6: Horizontal Load-Deflection Curve of Compression Wall, South Face

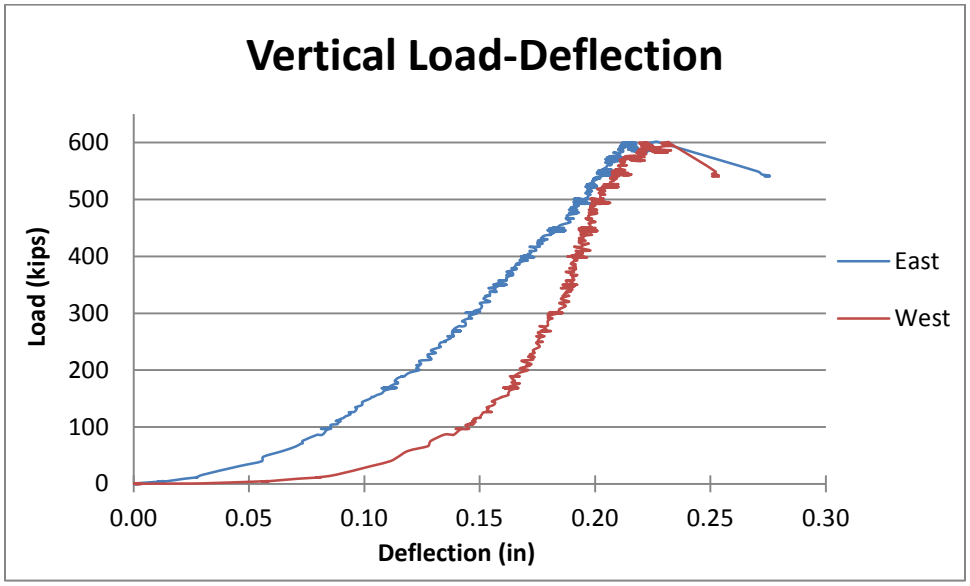

Figure C-7: Vertical Load-Deflection Curve of Compression Wall

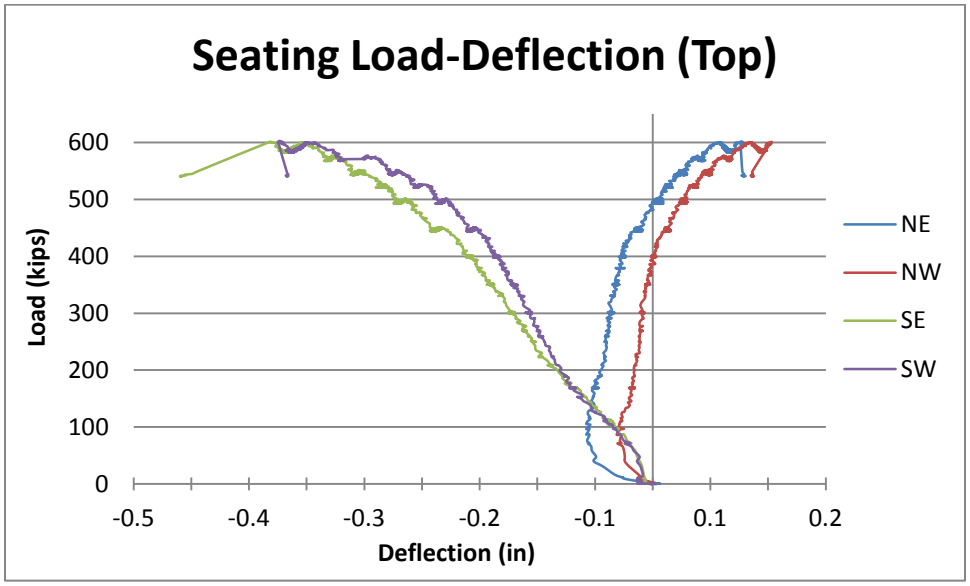

Figure C-8: Load-Deflection Curve of Seating of Top Beam of Compression Wall

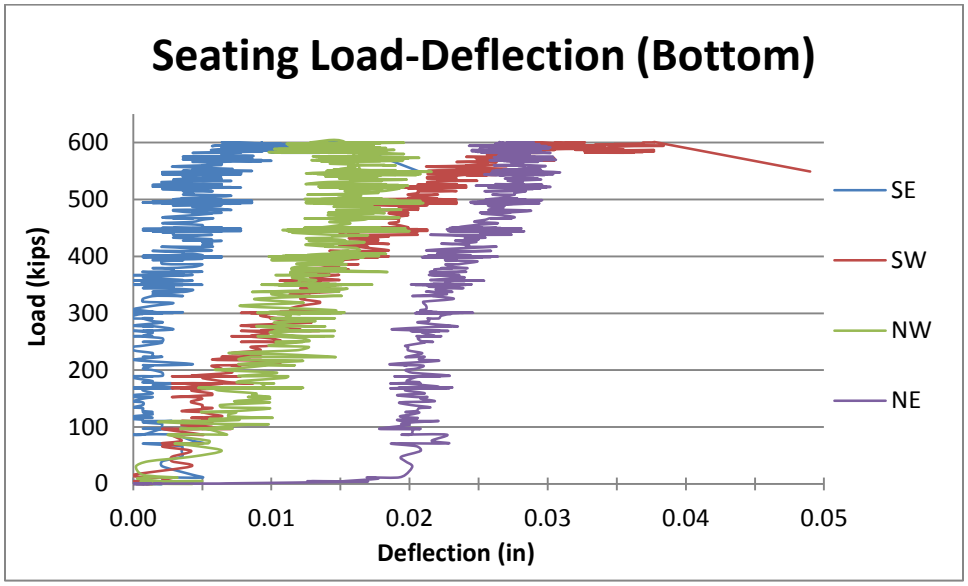

Figure C-9: Load-Deflection Curve of Seating of Bottom Beam of Compression Wall

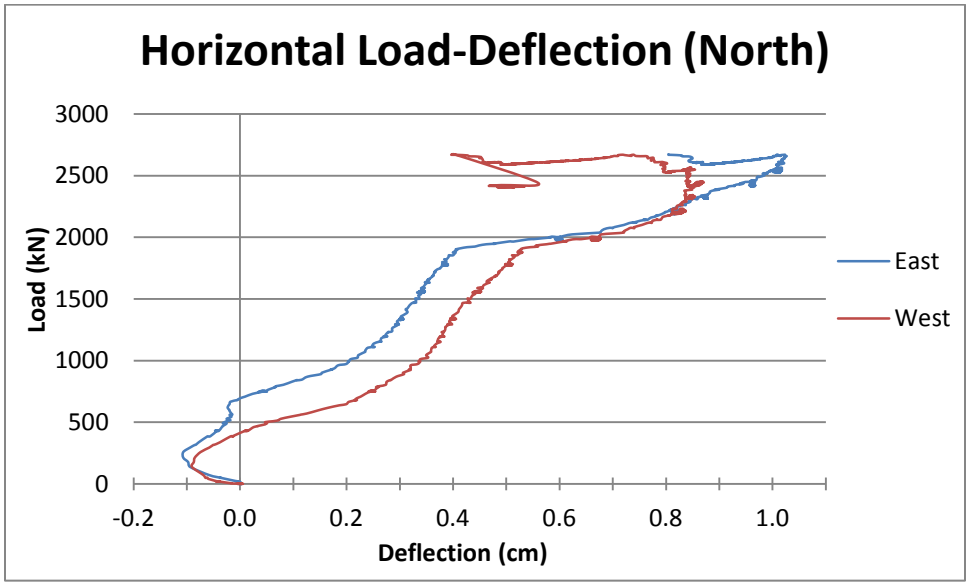

Figure C-10: Horizontal Load-Deflection of Compression Wall, North Face, SI Units

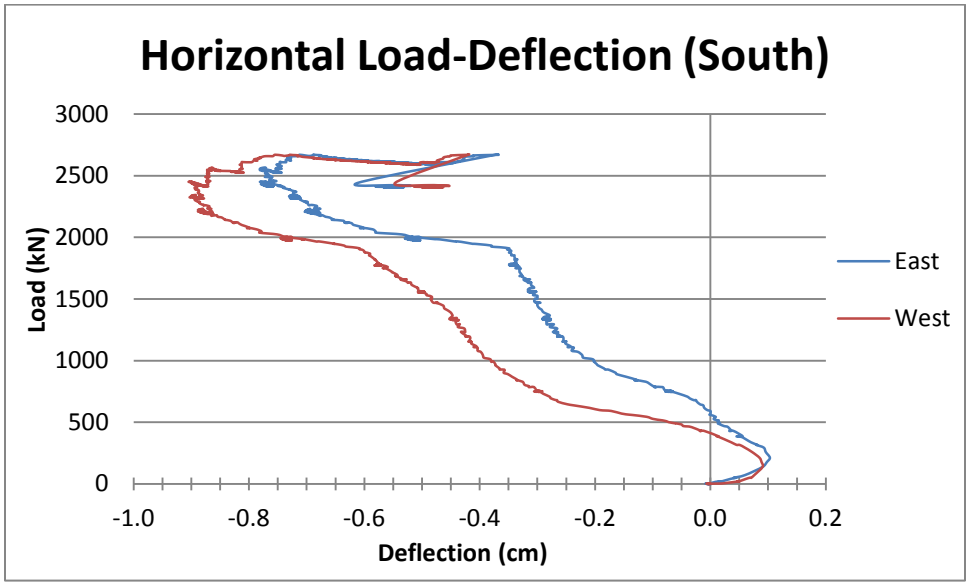

Figure C-11: Horizontal Load-Deflection of Compression Wall, South Face, SI Units

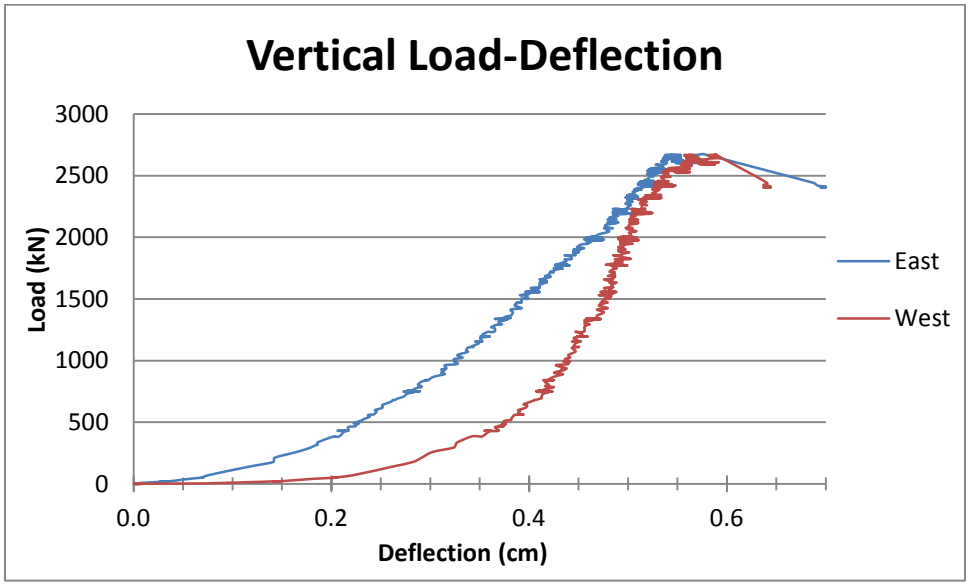

Figure C-12: Vertical Load-Deflection Curve of Compression Wall, SI Units

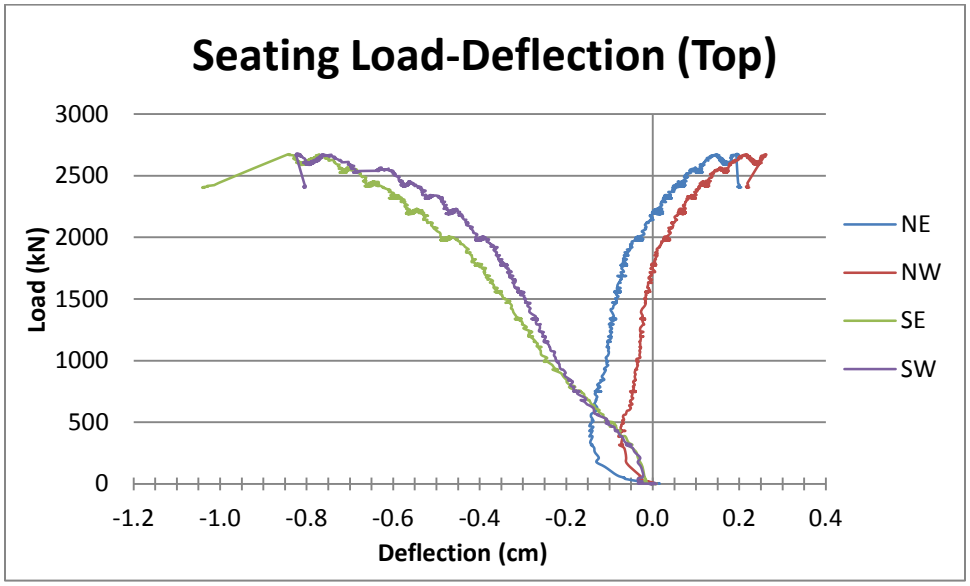

Figure C-13: Load-Deflection Curve of Top Beam of Compression Wall, SI Units

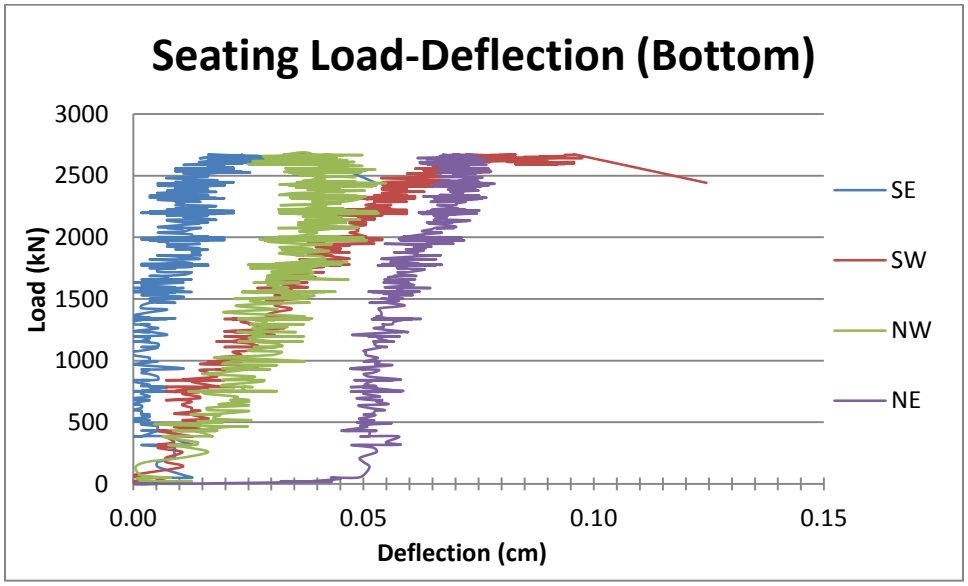

Figure C-14: Load-Deflection Curve of Bottom Channel of Compression Wall, SI Units

Table C-1: Measured and Calculated Strength Results of ICLT Panels, SI Units

	Racking Strength at Yield	Flexural Strength	Axial Strength
Calculated (kN)	20.0	270.4	3268.4
Measured (kN)	26.7	213.5	2673.2

APPENDIX D. CALCULATIONS

Step by step procedures of all calculations mentioned in the body of the thesis above.

Static Lateral Load on In-Plane Lateral Loading Wall

- 13kip Load on in-plane lateral load panel at 1.8in drift limit
- 8ft Length of wall parallel to load
- $L_s = \frac{13kip}{8ft}$=1.625kip/ft Static lateral load on in-plane lateral loading wall

Bending Stress on Out-of-Plane Loading Wall (looking at a 1ft width of wall)

- d=8.5in Thickness of ICLT panel
- h=1.5in Thickness of reduced cross section of outer member of ICLT panel
- l=90in Span length of ICLT panel
- b=12in 1ft width of ICLT panel section
- $y = \frac{d}{2}$ =4.25in Distance from centroid of panel to extreme fiber of outer layer of panel
- $I = 2\left(\frac{bh^3}{12} + bh\left(y - \frac{h}{2}\right)^2\right)$=447.8in^4 Moment of inertia of reduced cross section of 1ft width of ICLT panel

- a=30.128in Distance from support to line load of out-of-plane loading wall
- P=3kip Maximum line load applied to 1ft of ICLT panel
- $M = Pa$=90375in-lbf Maximum moment applied to 1ft ICLT panel
- $\sigma_b = \frac{My}{I}$=857.8psi Bending stress of reduced cross section of ICLT panel

Shear Stress on Out-of-Plane Loading Wall (looking at 1ft width of wall)

- h=1.5in Thickness of reduced cross section of outer member of ICLT panel
- b=12in 1ft width of ICLT panel section
- P=3kip Maximum line load applied to 1ft of ICLT panel
- $\tau = \frac{P}{2hb}$=83.3psi Shear stress of reduced cross section ICLT panel

Compressive Stress over Entire Cross Section of In-Plane Vertical Loading Wall

- P=601kip Maximum load applied to compression wall
- L=96in Length of the top of the wall
- d=8.5in Thickness of ICLT panel
- $\sigma_{ct} = \frac{P}{dL}$=736.5psi Compressive stress on gross cross section of compression wall

Compressive Stress on Vertical Members only, of In-Plane Vertical Loading Wall

- P=601kip Maximum load applied to compression wall
- L=96in Length of the top of the wall

- d=2.625in Thickness of ICLT panel
- $\sigma_{ct} = \frac{P}{2dL}$=1192.5psi Compressive stress on vertical members of compression wall

Calculations for Racking Strength Analytical Model

- F_{cp}=335psi #2 graded compression perpendicular to the grain strength, species type SPF South from Table 4A in NDS Supplement.
- C_M=1 Wet service factor, Adjustment factors for Table 4A in NDS supplement
- C_t=1 Temperature factor, Table 2.3.3 of NDS T≤100°F
- C_i=1 Incising factor, 4.3.8 of NDS, no incising
- l_b=3.75in Length of bearing area perpendicular to the grain
- $C_b = \frac{l_b+0.375}{l_b}$=1.1 Bearing area factor, equation3.10-2 in NDS
- φ_{cp}=0.9 Table N2, NDS
- λ=0.6 Table N3, NDS
- $K_{fb} = \frac{1.875}{\varphi_{cp}}$ Table N1, NDS
- $F_{cp}^{`} = F_{cp}C_M C_t C_i C_b \varphi_{cp} K_{fcp} \lambda$=414.6psi
    - NDS design compression perpendicular to the grain stress for #2 SPF South, Table4.3.1 NDS
- a=1.25in Distance from edge of vertical member to where crushing force is applied
- d_D=1in Depth of dovetail

- $A_c = l_b d_D$=3.75in2 Crushing area perpendicular to the grain
- $F_r = \frac{1}{2} A_c F_{cp}^{`}$=777.4lb Crushing force of vertical member on horizontal member
- b=5in Moment arm of crushing force
- $M = bF_r$=3887in-lbf Applied couple moment, Table 3-23 in Steel Construction Manual
- H=83in Distance between pin connections of ICLT racking wall
- n=(2,13) The number moment applied to the vertical member from interaction of the vertical and horizontal members binding at dovetail connections
- $V = \frac{nM}{H}$ Shear force applied to a single vertical member of the racking wall
    - V_2=93.7lbf Shear force when n=2
    - V_{13}=608.8lbf Shear force when n=13
- $R_T = \sum V$=4.5kips Total racking force applied to the in-plane lateral loading test at yeild

Calculations for Flexural Strength Analytical Model

- F_b=775psi #2 graded bending stress, species type SPF South from Table 4A in NDS Supplement.
- C_M=1 Wet service factor, Adjustment factors for Table 4A in NDS supplement
- C_t=1 Temperature factor, Table 2.3.3 of NDS T≤100°F
- C_L=1 Beam stability factor, 3.3.3.1 of NDS
- C_F=1 Size factor, Adjustment factors for Table 4A in NDS supplement, Width=8in and thickness=1.5in for reduced cross section from dovetail cut out

- C_{fu}=1 Flat use factor, Adjustment factors for Table 4A in NDS supplement, width 8in and thickness 1.5in for reduced cross section from dovetail cut out
- C_i=1 Incising factor, 4.3.8 of NDS, no incising
- C_r=1.15 Repetitive member factor, 4.3.9 of NDS
- φ_b=0.85 Table N2, NDS
- λ=0.6 Table N3, NDS
- $K_{fb} = \frac{2.16}{\varphi_b}$ Table N1, NDS
- $F_p^{`} = F_b C_M C_t C_L C_F C_{fu} C_i C_r \varphi_b K_{fb} \lambda$=1155psi
    - NDS design bending stress for #2 SPF South, Table4.3.1 NDS
- b=90in Span length of ICLT panel for out-of-plane loading test
- H=8.5in Full thickness of ICLT panel, used for solid beam calculations
- h=1.5in Thickness of single board from ICLT panel, minus the dovetail cut-out
- $d^{`} = \frac{H}{2} - \frac{h}{2}$ =3.5in Distance from centroid of 8.5in beam to centroid of 1.5in outer layer beam with middle void
- $S = \frac{bH^2}{6}$ =1083.7in^3 Section modulus of solid 8.5in beam
- $P = \frac{F^{`}_b S6}{b}$ =83.5kip Design capacity of solid 8.5in beam
- $I_s = \frac{bH^3}{12}$ =4606in^4 Moment of inertia for solid 8.5in beam
- $I_{iclt} = 2\left(\frac{bh^3}{12} + bhd^{`2}\right)$ =3358.1in^4 Moment of inertia of beam with middle void
- $R_I = \frac{I_{iclt}}{I_s}$ =0.729 Ratio of the two moments of inertia

- $P_{iclt} = R_I P$ =60.8kip Modeled flexural strength of ICLT panel

Calculations for Axial Compressive Strength Analytical Model

- F_b=1000psi #2 graded compression parallel to the grain stress, species type SPF South from Table 4A in NDS Supplement.
- C_M=1 Wet service factor, Adjustment factors for Table 4A in NDS supplement
- C_t=1 Temperature factor, Table 2.3.3 of NDS T≤100°F
- C_F=1.2 Size factor, Adjustment factors for Table 4A in NDS supplement, Width=8in and thickness=2.625in
- C_i=1 Incising factor, 4.3.8 of NDS, no incising
- E_{min}=400ksi Minimum modulus of elasticity, Table 4A of NDS supplement
- Ct=1 Buckling stiffness factor, 4.4.2 of NDS, Not a truss and members larger the 2x4
- φ_E=0.85 Table N2, NDS
- $K_{fE} = \frac{1.5}{\varphi_E}$ Table N1, NDS
- $E`_{min} = E_{min} C_M C_t C_i C_T K_{fE} \varphi_E$=600ksi
    - NDS design minimum modulus of elasticity, Table4.3.1 NDS
- $F_c^* = F_c C_M C_t C_F C_i \varphi_c K_{fc} \lambda$=1555psi Section 3.7.1 of NDS explanation for equation 3.7-1
- l_c=48in Unbraced length of vertical member in the weak axis, Figure 3F of NDS
- d=2.625in Vertical member thickness in the weak axis, Figure 3F of NDS
- b=7.5in Width of vertical member

- $I = \frac{bd^3}{12}$=11.3in^4 Moment of inertia of vertical member
- l_b=48in Unbraced length of beam section of vertical member in weak axis
- $G_A = \frac{\sum(EI/l)_c}{\sum(EI/l)_b}$=1 G factor of top joint, Page 16.1-240 in Steel Construction Manual
- $G_B = \frac{\sum(EI/l)_c}{\sum(EI/l)_b}$=1 G factor of bottom joint, Page 16.1-240 Steel Construction Manual
- Ke=0.55 Effective length factor from Figure C-C2.3 in Steel Construction Manual
- $l_e = l_c K_e$=26.4in Effective column length, section 3.7.1.2 of NDS
- $F_{cE} = \frac{0.822\grave{E}_{min}}{(l_e/d)^2}$=4876.1psi Section 3.7.1 of NDS, explanation for equation 3.7-1
- c=0.8 Section 3.7.1 of NDS, explanation for equation 3.7-1, sawn lumber
- $C_p = \frac{1+(F_{cE}/F_c^*)}{2c} - \sqrt{\left(\frac{1+(F_{cE}/F_c^*)}{2c}\right)^2 - \frac{F_{cE}/F_c^*}{c}}$=0.923
    - Column stability factor, equation 3.7-1 of NDS
- φ_b=0.9 Table N2, NDS
- λ=0.6 Table N3, NDS
- $K_{fc} = \frac{2.16}{\varphi_b}$ Table N1, NDS
- $\grave{F_c} = F_c C_M C_t C_F C_i C_p \varphi_c K_{fc} \lambda$=1435.4psi
    - NDS design compression parallel to the grain strength for #2 SPF South, Table4.3.1 NDS

- $A_v = bd$=19.7in^2 Cross sectional area of a vertical member
- $P_c = F_c` A_v$=734.8kip Axial compressive strength of ICLT in-plane vertical loaded wall

Tension Perpendicular to the Grain Strength of Dovetail

- F_{tp}=290psi Tension perpendicular to the grain strength, Table 5-3b of Wood Handbook, Lodgepole Pine
- w_D=5in Width of dovetail on dovetail members
- l_D=45in Length of horizontal dovetail that was fractured
- $P_D = w_D l_D F_{tp}$=65.25kip Tension perpendicular to the grain strength of horizontal dovetail member in compression wall